Mangrove microbiota along the urban-to-rural gradient of the Cayenne estuary (French Guiana, South America): Drivers and potential bioindicators

Maud Fiard, Philippe Cuny, Léa Sylvi, Cédric Hubas, Ronan Jézéquel, Dominique Lamy, Romain Walcker, Amonda El Houssainy, Lars-Eric Heimbürger-Boavida, Tony Robinet, et al.

Mangrove microbiota along the urban-to-rural gradient of the Cayenne estuary (French Guiana, South America): drivers and potential bioindicators

Maud Fiard[a*], Philippe Cuny[a], Léa Sylvi[a], Cédric Hubas[b], Ronan Jézéquel[c], Dominique Lamy[d], Romain Walcker[e], Amonda El Houssainy[a], Lars-Eric Heimbürger-Boavida[a], Tony Robinet[b], Isabelle Bihannic[f], Franck Gilbert[e], Emma Michaud[f], Guillaume Dirberg[g], and Cécile Militon[a]

[a] Aix Marseille Univ., Université de Toulon, CNRS, IRD, MIO, 13288 Marseille, France; philippe.cuny@mio.osupytheas.fr (P.C.); lea.sylvi@mio.osupytheas.fr (L.S.); amonda.houssainy@gmail.com (A.E.H.); lars-eric.heimburger@mio.osupytheas.fr (L.-E.H.-B.); cecile.militon@mio.osupytheas.fr (C.M.).

[b] Biologie des Organismes et Ecosystèmes Aquatiques (UMR 8067 BOREA) Muséum National D'Histoire Naturelle, CNRS, Sorbonne Université, IRD, UCN, UA, Station Marine de Concarneau, 29900 Concarneau, France; cedric.hubas@mnhn.fr (C.H); tony.robinet@mnhn.fr (T.R).

[c] CEDRE, Rue Alain Colas, 29218 Brest CEDEX 2, France; ronan.jezequel@cedre.fr (R.J.).

[d] Institute of Ecology and Environmental Sciences of Paris (iEES-Paris), Sorbonne Université, Univ Paris Est Créteil, IRD, CNRS, INRA, 4 place Jussieu, 75005 Paris, France; dominique.lamy@sorbonne-universite.fr (D.L).

[e] Laboratoire Ecologie Fonctionnelle et Environnement, Université de Toulouse, CNRS, Toulouse, France; romain.walcker@univ-tlse3.fr (R.W.); franck.gilbert@univ-tlse3.fr (F.G.).

[f] Univ Brest, CNRS, IRD, Ifremer, LEMAR, 29280 Plouzané, France; isabelle.bihannic@univ-brest.fr (I.B.); emma.michaud@univ-brest.fr (E.M).

[g] Biologie des Organismes et Ecosystèmes Aquatiques (UMR 8067 BOREA) Muséum National D'Histoire Naturelle, CNRS, Sorbonne Université, IRD, UCN, UA, Rue Buffon, 75005 Paris, France; guillaume.dirberg@mnhn.fr (G.D.).

*Correspondance : maud.fiard@mio.osupytheas.fr; Tel. : +33486090512.

Keywords: Estuarine mangrove sediments, French Guiana, low organic matter enrichment, organochlorine contaminants, PAHs contamination

Abstract:

The microbial communities inhabiting the Atlantic-East Pacific (AEP) mangroves have been poorly studied, and mostly comprise chronically polluted mangroves. In this study, we characterized changes in the structure and diversity of microbial communities of mangroves along the urban-to-rural gradient of the Cayenne estuary (French Guiana, South America) that experience low human impact. The microbial communities were assigned into 50 phyla. Proteobacteria, Chloroflexi, Acidobacteria, Bacteroidetes, and Planctomycetes were the most abundant taxa. The environmental determinants found to significantly correlated to the microbial communities at these mangroves were granulometry, dieldrin concentration, pH, and total carbon (TC) content. Furthermore, a precise analysis of the sediment highlights the existence of three types of anthropogenic pressure among the stations: (i) organic matter (OM) enrichment due to the proximity to the city and its wastewater treatment plant, (ii) dieldrin contamination, and (iii) naphthalene contamination. These forms of weak anthropogenic pressure seemed to impact the bacterial population size and microbial assemblages. A decrease in Bathyarchaeota, "*Candidatus* Nitrosopumilus", and *Nitrospira* genera was observed in mangroves subjected to OM enrichment. Mangroves polluted with organic contaminants were enriched in Desulfobacteraceae, Desulfarculaceae, and Acanthopleuribacteraceae (with dieldrin or polychlorobiphenyl contamination), and Chitinophagaceae and Geobacteraceae (with naphthalene contamination). These findings provide insights into the main environmental factors shaping microbial communities of mangroves in the AEP that experience low human impact and allow for the identification of several potential microbial bioindicators of weak anthropogenic pressure.

Significance and impact of the study:

- The spatial variation of mangrove microbiota is studied in relation to environmental factors and contaminants in the Cayenne estuary (French Guiana).
- Cayenne estuary mangroves are globally pristine, but low-level human pressures were detected (OM enrichment and NOAA ERL thresholds exceeded for naphthalene and dieldrin).
- pH, dieldrin, TC, and granulometry are the main drivers influencing the profile of the microbial community.
- Bathyarchaeota, "*Candidatus* Nitrosopumilus*"*, and *Nitrospira* were identified as potential indicators of OM enrichment in mangroves.
- Polluted mangroves were enriched in Deltaproteobacteria, Acidobacteria, Chitinophagaceae, and Geobacteraceae.

1. Introduction

Tropical and subtropical intertidal zones are occupied by iconic mangrove forests ecosystems, extending approximately 137,000 km² along the shores of 123 countries (Bunting et al., 2018). Within latitudes of around 32°N and 38°S, mangroves harbor significant biodiversity distributed in two distinct floristic realms (Spalding, 2010), the AEP and the Indo–West Pacific (IWP) (Duke, 1992). These forests are assemblages of salt-tolerant trees and shrubs that grow on soft sediments in places where freshwater mixes with seawater (e.g., estuarine margins and coastal marine environments). Mangroves are well adapted to dynamic environments (salinity fluctuations, periodic flooding, and anoxia of sediment) and are among the most productive ecosystems in tropical coastal areas (Donato et al., 2011). They carry out functions of great ecological importance (e.g., carbon and nutrient recycling, provision of breeding and feeding areas), and they also provide valuable ecosystem services such as coastal protection (Massel et al., 1999) and climate change mitigation (Laffoley and

Grimsditch, 2009; Walcker et al., 2018). Despite the numerous services they provide, mangroves are being degraded by anthropogenic activities and lost at an alarming rate in some areas (Carugati et al., 2018).

The benthic microbiota plays a fundamental role in mangrove functioning because it processes most of the energy flow and nutrients. It is responsible for OM degradation and nutrient recycling (Alongi, 1994). Mangrove microorganism biodiversity has been the subject of numerous studies, which have deepened our understanding of the microbial communities inhabiting the mangrove rhizosphere (Gomes et al., 2014) and mangrove sediments (Jiang et al., 2013; Mendes et al., 2012; Nogueira et al., 2015; Rocha et al., 2016; Santana et al., 2019). However, most of the studies were mainly focused on mangroves in the IWP region. Most of the studies conducted in the AEP region have been within the Eastern American subregion and dealt with coastal mangroves in southern Brazil (Dias et al., 2010, 2011; Peixoto et al., 2011; Rigonato et al., 2013) and Colombia (Torres et al., 2019). In these countries, the anthropogenic pressure on mangroves is very strong in some areas due to the proximity of big industrial cities and sites of offshore oil exploitation. Because microorganisms are stress-sensitive, several microbial bioindicators of pollution were identified in Brazilian and Colombian mangroves (Peixoto et al., 2011; Torres et al., 2019).

Apart from chemical contaminants (Matturro et al., 2016; Sheng et al., 2016, Zhang et al 2014), the microbial structure and composition of prokaryotic communities in soils and sediments are known to be shaped by several physicochemical factors such as carbon and nitrogen concentration (Liu et al 2012), redox potential (DeAngelis et al 2010), pH (Aciego Pietri and Brookes, 2008; Wardle, 1992), and salinity (Chambers et al 2016). Compared to the IWP mangroves and the human-impacted AEP mangroves, relatively little is known about the factors shaping the distribution of the microbial communities in low-human impacted AEP mangroves. Within the Eastern American subregion of the AEP zone, the mangrove coastline

of the Guianas (between the Oyapock and Orinoco Rivers estuaries) appears to be an exception, as the mangroves here experience low-level human impact (Diop et al., 2016; Michelet et al., 2021). In French Guiana (FG), mangroves occupy about 80% of the coastal line with a total extent of about 70,000 ha (Fromard, Vega, and Proisy 2004). Due to their localization, near the Amazon's mouth (Brazil), FG mangroves are very dynamic and are under the influence of one of the world's largest sediment discharge systems (Anthony et al., 2010; Marchand et al., 2006).

In order to better understand which environmental drivers are important to explain the compositional changes of mangrove microbiota in the AEP, an analysis of the microbial diversity in Guiana's mangroves was carried out.

Based on the same sedimentary cores used by Michelet et al. (2021) and considering the different sedimentary layers, we assessed the microorganism response to low human pressure along the Cayenne estuary and defined the main environmental drivers shaping the structure and diversity of communities.

Finally, an exploration of the changes in the relationship between mangrove microbiota diversity and the abiotic environment, according to sediment depth and the urban-to-natural gradient, allowed us to identify potential microbial bioindicators of mangrove health.

2. Materials and Methods

2.1. Study area and sampling strategy

The location of the study area was the Cayenne estuary in FG (South America; Figure 1). Three stations (S1, S2, and S3) were selected on the edge of the estuary (<5 m) and at an increasing distance from Cayenne city, which is the largest city and the capital of FG (61,268 inhabitants; INSEE 2017), along an urban-to-natural gradient. Station 1 (S1) is located at the Crique Fouillée tributary creek (4°54'53.208" N, 52°20'15.9324" W; Figure 1), draining

urban waters and the effluents of the wastewater treatment plant of Cayenne city (urban, commercial, and industrial waters). Station 2 (S2) is located near the confluence of the Cayenne and Montsinery Rivers, which flow in the Cayenne estuary (4°53'49.2288" N, 52°22'27.714" W; Figure 1). This station receives water from the suburban Cayenne drainage basin. Station 3 (S3) is located southeast of Cayenne city, 11.7 km from S1 and 4.7 km from S2, along the Cayenne River (4°51'31.9716" N, 52°23'59.5248" W; Figure 1) in a natural area farther from human activities.

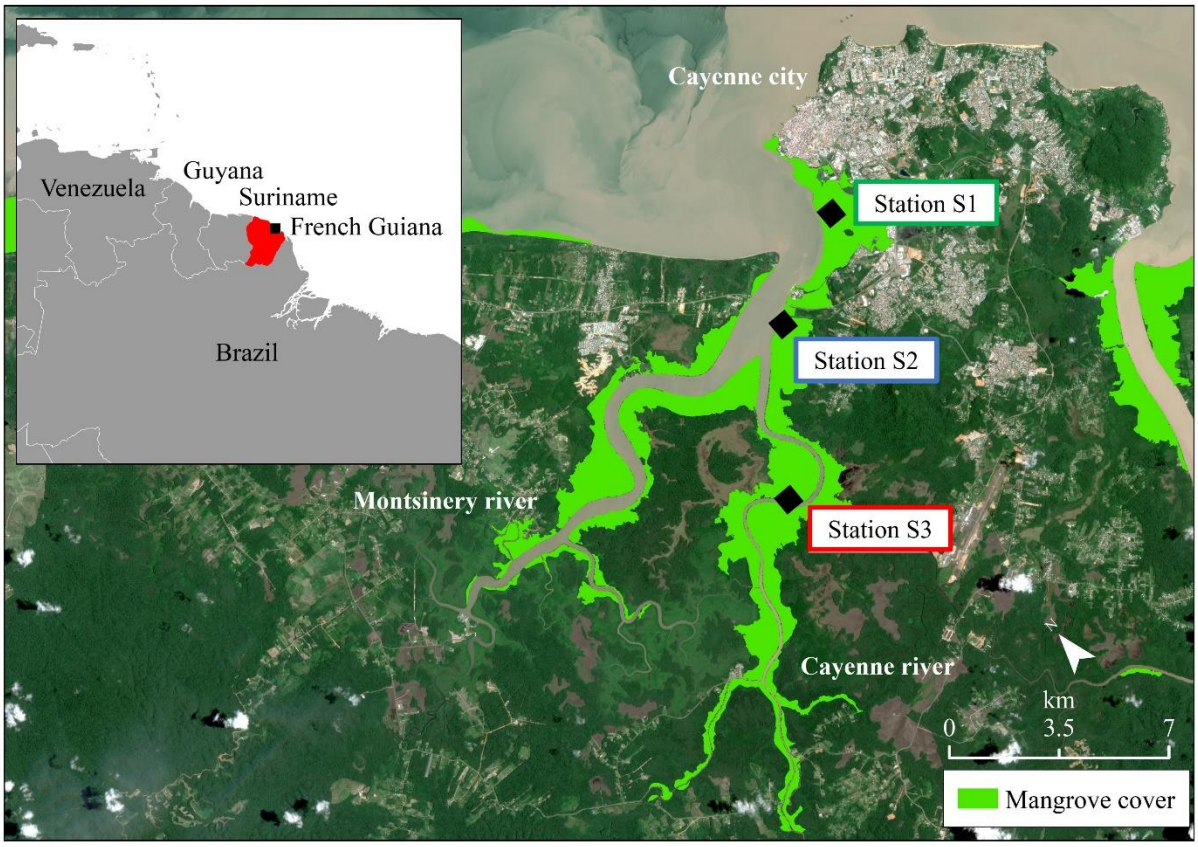

Figure 1. Location of mangrove sampling stations in FG (South America). S1 is located near Cayenne city, S2 at the confluence of Cayenne and Montsinery Rivers, and S3 along the Cayenne River. Mangrove cover is represented in green. (modified from Michelet et al., 2021).

At each station, three sediment cores (A, B and C) were collected at low tide, within a 10 m^2 plot and located 2 m away from each other, with plexiglass tubes (internal diameter 10.4 cm, height 20 cm) between November 19 and 21, 2017 (spring tides, dry season). The

sediment cores were sliced in 0.5 cm thick layers around the two first centimeters, then 1 cm thick layers until the end of the core. The obtained layers were randomly subsampled to create 3 pools of sediments: 0 to 2 cm, 2 to 10 cm, and 10 cm to the end of the core.

During subsampling, the pH and redox potential (Eh) were immediately measured with a multiparameter probe (WTW Multi 3500i). The slices were then subsampled for characterization of environmental parameters: granulometry, TC, total nitrogen (TN), trace metals and metalloids (TMM), organic contaminants, and microbial analysis. Subsamples were immediately frozen and stored at −80 °C (for TC, TN, TMM, organic contaminants, and microbial analyses) or 4 °C (for granulometry analysis).

2.2. Treatment

2.2.1. Measurement of TC and TN and determination of granulometry

Sediments were freeze-dried over 24 h, crushed to powder, and homogenized for sediment analysis. TC and TN were measured by combustion at 930 °C using a CHN carbon analyzer (Flash-2000; Thermo Fisher Scientific Inc., Milan, Italy). In FG, the total organic carbon and TC appeared to be very well correlated, due to the lack of carbonates (Marchand et al., 2004). Thus, TC can be considered as a proxy for carbon organic content in the sediments. Granulometry analysis was realized using a laser beam diffraction analyzer (Partica LA-950V2; Horiba Instruments, Inc.).

2.2.2. Contaminants and TMM analysis

Five groups of organic contaminants—15 polycyclic aromatic hydrocarbons (PAHs), some of which are frequently monitored according to recommendations by the European Union and the US Environmental Protection Agency (acenaphthene, acenaphthylene, anthracene, benzo[ghi]perylene, benzo[a]anthracene, benzo[b]fluoranthene,

benzo[b+k]fluoranthene, benzothiophene, biphenyl, chrysene, dibenzothiophene, fluoranthene, fluorene, naphthalene, phenanthrene, and pyrene), 11 polychlorinated biphenyls (PCB-7, PCB-28, PCB-52, PCB-101, PCB-105, PCB-118, PCB-138, PCB-153, PCB-156, PCB-169, and PCB-180), 12 organochlorine pesticides (2,4-DDT, 2,4-DDD, 2,4-DDE, 4,4-DDD, 4,4-DDE, 4,4-DDT, aldrin, chlordecone, dieldrin, endrin, hexachlorobenzene (HCB), and isodrin), 6 phthalates (DMP, DEP, DBP, BBP, DEHA, and DEHP), and 7 polybromodiphenylethers (BDE 28, BDE 47, BDE 99, BDE 100, BDE 153, BDE 154, and BDE 183) were extracted from the sediments and analyzed (Michelet et al., 2021). For PAHs, PCB, and pesticides quantification, naphthalene d_8, biphenyl d_{10}, phenanthrene d_{10}, pyrene d_{10}, chrysene d_{12}, benzo(a)pyrene d_{12}, benzo(g,h,i)perylene d_{12} were used as standards. For the plastic additives, di (2-ethylhexyl) phthalate- d_4 and BDE 77 were respectively used as standards. All standards were obtained from LGC Standard (Wesel, Germany) and Interchim (Montluçon, France). In order to discriminate the sources of PAHs, the ratios Flt/(Flt + Pyr) and Ant/(Ant/Phe) (Flt, fluoranthene; Pyr, pyrene; Ant, anthracene; Phe, phenanthrene) were calculated and compared to the published cut-off values (at > 0.5, PAHs are likely to occur from biomass burning) (Brändli et al., 2007; Katsoyiannis et al., 2007).

Twenty-seven TMM were quantified in each sample such as lead (Pb), chromium (Cr), nickel (Ni), copper (Cu), zinc (Zn), manganese (Mn), mercury (Hg), arsenic (As) and molybdenum (^{95}Mo). Extraction and analysis protocols are presented in detail in Michelet et al. (2021). To check the accuracy of the TMM measurements, the certified reference material MESS-4 (National Research Council Canada) was run before starting the measurements and many times per analytical batch (Supplementary Data A). The analytical recovery was within 10% compared to certified concentration. Freeze-dried sediment (Christ Gamma 1-16 LSCplus) were analyzed for particulate Hg using a CV-AAS (LECO AMA 254) equipped with a low Hg optical cell. The method detection limit was 2 pg (3 times the standard

deviation of the blank samples). The measured values were always within ± 5% of the recommended values.

2.2.3. Total DNA extraction and quantification

Sediments were freeze-dried for 48 h and crushed to powder using a sterilized mortar and pestle. Total DNA was then extracted from 0.25-0.30 g dry sediment with the DNeasy PowerSoil Kit (Qiagen) according to the manufacturer's protocol. The DNA extracts were quantified by fluorometric dosage with a Quantifluor dsDNA system kit (Promega) according to the supplier's recommendations. The total DNA measurement (molecular microbial biomass) was used as a proxy for the microbial biomass.

2.2.4. Quantitative polymerase chain reaction (qPCR)

To determine the bacterial and archaeal abundances in the sediments, 16S rRNA genes (*rrs*) were quantified by qPCR. The GoTaq qPCR Master Mix (Promega) was used following the supplier's recommendations, using specific archaeal (931F: 5'-AGGAATTGGCGGGGGAGCA-3' and m1100R: 5'-BTGGGTCTCGCTCGTTRCC-3') and bacterial (300F: 5'-GCCTACGGGAGGCAGCAG-3' and univ516R: 5'-GTDTTACCGCGGCKGCTGRCA-3') primer sets (for a review, see Klindworth et al., 2013). The qPCR cycles for archaea consisted of initial denaturation (3 min at 98 °C), followed by 35 cycles of denaturation for 10 s at 98 °C, primer hybridization for 10 s at 62 °C, and elongation for 20 s at 72 °C. For bacteria, the first step of initial denaturation lasted 2 min at 98 °C, followed by 30 cycles of initial denaturation for 5 s at 58 °C, primer hybridization for 10 s at 55 °C, and elongation for 12 s at 72 °C.

2.2.5. 16S rRNA gene amplification and sequencing

To characterize the structure and composition of the bacterial and archaeal communities, hypervariable regions V4–V5 of the 16S rRNA genes were amplified by PCR using the 515f (5'-TGT GYC AGC MCG CGC GGT A-3') and 928r (5'-CCG YCA ATT CMT TTR AGT-3') primer sets (Parada et al., 2016). Each 25 µL reaction mix contained 2 µL of DNA (~0.5–5 ng μL^{-1}), 10 µM of 515f forward primer, 10 µM of 928r reverse primer, 10 mM of dNTPs, 0.4 µL of Pfu DNA polymerase (Promega), and 2.5 µL of Pfu buffer (Promega). The PCR cycles consisted of initial denaturing for 2 min at 94 °C, followed by 35 cycles composed of denaturation for 20 s at 94 °C, primer hybridization for 20 s at 50 °C, and elongation for 25 s at 72 °C in a T100 thermal cycler (Bio-Rad). PCR products were verified by agarose gel electrophoresis (1.5% w/v). Amplicon purification was performed using the Agencourt AMPure XP system, and quantification, with QuantIT PicoGreen. Primers containing the Illumina adapters flanked by floating tails complementing those on amplicons and 5 µL of purified amplicons were added for the second round of amplification. The PCR cycling started at 94 °C for 2 min, followed by 12 cycles of amplification (94 °C for 1 min, 55 °C for 1 min, 68 °C for 1 min), and a final extension step at 68 °C for 10 min. The purified amplicons were sequenced on an Illumina MiSeq platform (Genotoul, Toulouse, France).

2.2.6. Sequence analysis

The raw data were processed using the dada2 package (v.3.9) in R studio interface (v3.2.3) following the workflow described by Callahan et al. (2016). The raw sequence datasets are available in the National Center for Biotechnology Information database under the PRJNA735070 BioProject. For taxonomic assignment, amplicon sequence variants (ASVs) were compared with the Silva database (Silva v_132) (Quast et al., 2013). All non-assigned reads at the phylum level and reads belonging to chloroplasts and mitochondria were removed from the dataset. To compare the diversity index (specific richness and Shannon

index), the samples were rarefied at an even number of sequences (4180 reads) with the phyloseq package (v3.9) (McMurdie and Holmes, 2013).

2.2.7. Statistical analysis

Statistical analyses were performed with R studio software (v3.2.3). As described by Michelet et al. (2021), a multiple factor analysis (MFA) (Escofier and Pagès, 1994) constituted by four variable groups (physicochemical parameters, OM, organic contaminants, and TMM) was performed using FactoMineR (Lê et al., 2008) and factoextra (Kassambara and Mundt, 2020) packages to compare microbiota and environmental parameters in the three stations and depths (statistical individuals). Only variables with a large contribution to one of the axes ($cos^2 > 0.5$) were plotted (Figure 2). Differences in environmental parameters and relative abundance of each taxonomic group were tested and displayed by the Scheirer–Ray–Hare test and Wilcoxon pairwise test in the R companion package (Mangiafico, 2021). A forward selection and a permutation test (vegan package) (Oksanen et al., 2020) were performed on the noncollinear variables (lattice package) (Sarkar, 2008) to determine the environmental drivers of the microbial community composition. This selection was followed by permutational multivariate analysis of variance (PERMANOVA) in the vegan package in order to test the differences in prokaryotic composition between samples. The top 30 phyla Z-scores were calculated in the ComplexHeatmap package (Gu et al., 2016), and these analyses were completed with pairwise Spearman correlation (r_s) to determine the correlations between taxa and environmental factors.

3. Results and discussion

3.1. Sampling stations characteristics and specificities

The physicochemical parameters (pH, Eh, granulometry), organic matter characteristics (TC, TN, TC:TN), TMM levels, and organic contaminant concentrations of sediments from

three sampling sites (S1, S2, and S3) and three depths (0-2, 2-10, and > 10 cm) are recorded in Table 1 and in Supplementary Tables B. In addition, multivariate analysis (MFA) was used to determine the sediment characteristics and specificities (Figure 2).

Axis 1 shows a separation between stations, mainly explained by variations in granulometry, TC, TN, TC:TN, and TMM concentrations (Figure 2B). All sediments were dominated by the silt fraction (74-89%), but a higher sand value is shown for S1 (18-21%; $p > 0.05$), situated closer to the ocean (Figure 2B, Supplementary Data B). At this station, higher TC (2-6%) was also measured ($p < 0.001$; Figure 2B; Supplementary Data B), while the TC levels in the sediment at S2 and S3 (1-2%) were lower and similar to those of nearby mangroves (Marchand et al., 2006). A slight enrichment in nitrogen was also observed in the surficial sediment at S1 (TN ~0.3%; Figure 2B, Supplementary Data B). The slight OM enrichment observed was likely due to the proximity with Cayenne city (urban runoff) and its wastewater treatment plant. Higher TC:TN ratios were also observed at S1 at all depths (15.1 to 17.9; $p < 0.001$; Figure 2B, Supplementary Data B). This ratio is usually used as a proxy to determine the source and fate of OM in water (e.g., Gordon and Goni, 2003; Ramanathan et al., 2008; Wu et al., 2007). The measured values in S1 are in line with TC:TN ratio generally observed for terrigenous OM (e.g., mangrove tree leaves and roots), which is known to be poorly degradable by microorganisms (Marchand et al., 2003). The OM characteristics (TN, TC, and TC:TN ratio) were very similar at S2 (10.3 ± 1.2) and S3 (9.5 ± 0.4). S1 was also characterized by 1.2 times higher Hg concentration than the two other stations ($p < 0.01$; Table 1, Figure 2B). A positive correlation was found between Hg and TC ($r_s = 0.76$; $p < 0.001$). Previous studies have shown that OM content probably promotes Hg storage in mangrove sediments (Marchand et al., 2006; Lei et al., 2019).

298 **Table 1.** Levels of organic contaminants and metals in sediments at three depths (0-2, 2-10, > 10 cm) at three sampling stations (mean ± SD, n =
299 3). Bold numbers correspond to values superior to OSPAR ERL or NOAA threshold.
300

	Station 1			**Station 2**			**Station 3**		
Depth	**0-2 cm**	**2-10 cm**	**>10 cm**	**0-2 cm**	**2-10 cm**	**>10 cm**	**0-2 cm**	**2-10 cm**	**>10 cm**
	Organic contaminants concentrations (ng g^{-1} d.w.)								
ddd24	0.1 ± 0.1	0	0.3 ± 0.3	0.3 ± 0.5	0.2 ± 0.1	0.5 ± 0.5	0	0	0
dde44	0.1 ± 0.1	0	0.3 ± 0.3	0.1 ± 0.2	0.2 ± 0.2	0.2 ± 0.3	0	0	0
DBT	0	2.8 ± 3.9	2.4 ± 4.2	4.4 ± 7.6	2.4 ± 4.1	10.1 ± 17.4	11.2 ± 12.6	1.4 ± 2.4	6.4 ± 1.6
Dieldrin	1.6 ± 0.3	1.7 ± 0.3	1.8 ± 0.3	1.9 ± 0.2	1.9 ± 0.3	**2.0 ± 0.1**	0	0	0
HCB	1.1 ± 1.0	0.7 ± 0.1	1.4 ± 0.9	1.9 ± 2.2	0.6 ± 0.4	2.8 ± 2.6	0	0	0
Naphthalene	0	0	0	0	28.1 ± 48.6	**227.5 ± 394.1**	**274.1 ± 191.6**	**110.5 ± 33.6**	**232.2 ± 33.4**
PCBs	1.2 ± 0.5	1.1 ± 0.1	2.2 ± 0.9	1.4 ± 4.3	3.2 ± 0.9	3.4 ± 3.0	0.1 ± 0.1	0	0
Phenanthrene	8.5 ± 1.2	12.5 ± 5.0	6.7 ± 6.9	7.3 ± 4.8	8.1 ± 5.1	14.1 ± 13.5	17.0 ± 18.9	6.0 ± 1.6	9.3 ± 1.3
	TMM concentrations (µg g^{-1} d.w.)								
Al (mg g^{-1})	109.3 ± 5.8	113.2 ± 1.5	107.8 ± 5.0	115.8 ± 3.7	115.0 ± 3.7	114.7 ± 6.0	118.3 ± 1.5	117.9 ± 0.5	116.9 ± 6.0
^{111}Cd	0.09 ± 0.02	0.08 ± 0.01	0.08 ± 0	0.07 ± 0	0.07 ± 0.01	0.07 ± 0	0.07 ± 0	0.06 ± 0	0.07 ± 0
Cr	78.1 ± 5.0	82.5 ± 3.5	77.2 ± 4.5	**84.4 ± 3.6**	**84.3 ± 2.3**	**84.9± 4.4**	**87.5 ± 1.4**	**87.7 ± 0.5**	**87.2 ± 4.5**
Hg (ng g^{-1})	64.2 ± 5.0	56.3 ± 2.3	57.5 ± 4.4	44.7 ± 0.8	48.4 ± 1.2	47.9 ± 0.3	48.8 ± 1.3	53.2 ± 0.6	50.9 ± 3.4
Mn	436.7 ± 44.0	434.4 ± 225.6	424.3 ± 68.4	1328.4 ± 404.2	696.7 ± 291.3	560.0 ± 80.0	1136.6 ± 100.5	999.2 ± 227.2	840.0 ± 224.3
^{95}Mo	2.6 ± 0.2	1.8 ± 0.1	1.9 ± 0.6	1.2 ± 0.2	1.5 ± 0.3	1.2 ± 0.1	1.3 ± 0.1	1.6 ± 0.1	1.4 ± 0.1
Zn	131.7 ± 13.3	149.20 ± 4.18	134.5 ± 14.2	149.4 ± 5.2	147.8 ± 6.8	146.6 ± 8.0	**160.2 ± 4.2**	**154.0± 2.6**	**152.4 ± 6.8**

301 The Hg concentrations measured in the Cayenne estuary correspond to natural background
302 levels observed in mangrove estuarine sediments in FG (Marchand et al., 2006) and were
303 below the NOAA ERL sediment quality guidelines (low effects range) (Burton, 2002). The
304 concentrations of ^{95}Mo (2.6-1.8 µg g^{-1}) and ^{111}Cd (0.07-0.08 µg g^{-1}) were also higher at S1 ($p < 0.001$; Table 1, Figure 2B). On the contrary, Cr, Zn, Al, and Mn concentrations were lower
306 at S1 ($p < 0.01$). At S2 and S3, the Cr content (84.5 µg g^{-1}) was slightly higher than the
307 NOAA ERL values (80 µg g^{-1}) (Burton, 2002) and higher than the range already observed in
308 FG (Marchand et al., 2006). At S3, the Zn concentration (155.5 µg g^{-1}) in the sediments was
309 also slightly higher than the ERL value (150 µg g^{-1}). As concluded by Marchand et al. (2006),
310 even if the origin of metals is difficult to clearly define, metals in FG mangrove sediments
311 most probably result from diagenetic processes rather than anthropogenic inputs. Observed
312 differences between stations are probably related to the differences in granulometry (e.g., sand
313 content) and TC contents.
314 The second axis of the MFA discriminated the samples based on pH, redox potential, and
315 organic contaminant concentration (Figure 2B). The pH of sediment pore water was 6.2 on
316 average (min 5.7, max 6.5), but clear differences in pH profiles were observed between
317 stations. Notably, pH gradients existed within the sedimentary columns at S1 and S3, where
318 increases and decreases greater than 0.5 pH units were observed, respectively. The sediments
319 were dominated by aerobic redox conditions in S1 and S3 (Eh ~100-200 mV) and were more
320 reduced in S2 (Eh ~-100 mV) (Figure 2B, Supplementary Data B). Significant differences in
321 pesticide, PCB, and PAH concentrations were also observed between stations ($p < 0.05$;
322 Figures 2B, 2D). Although organochlorine pesticides (HCB, ddd24, dieldrin) and PCBs were
323 detected at S1, the highest concentrations were observed at S2 (Table 1, Figure 2B). These
324 compounds are among the 12 most persistent organic pollutants (POPs) according to the

Stockholm Convention on POPs (2001) and are also listed as priority chemicals in the EU Water Framework Directive 2013/39/EC (European Union, 2013).

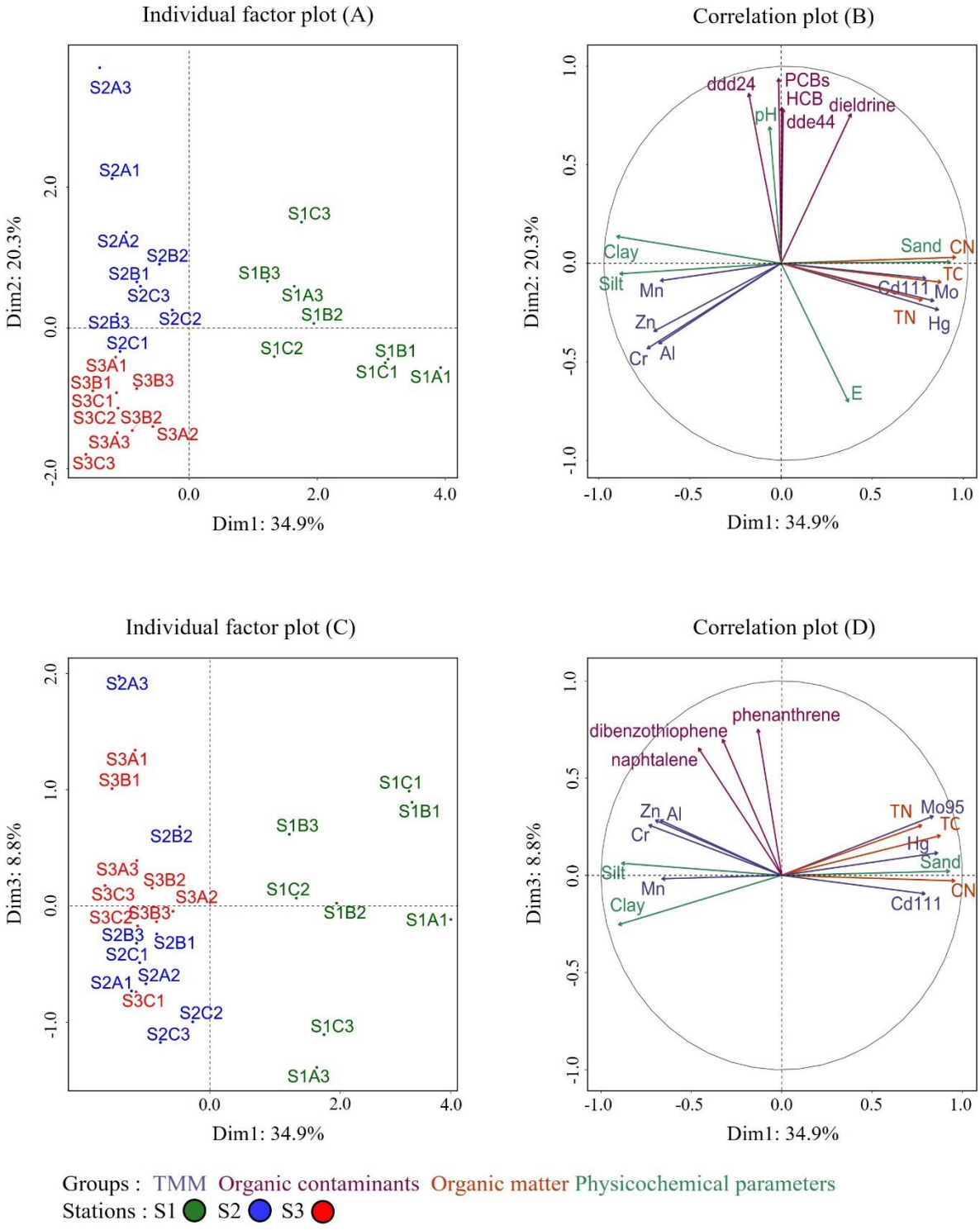

Figure 2. Multiple factor analysis of data obtained from different stations with four groups of variables (cos^2 > 0.5): physicochemical parameters (green), OM (orange), organic contaminants (purple), and TMM (blue). Graphs represent (A,C) individual factor plots and

(B,D) correlation plots on axes 1 and 2 (A,B) and 1 and 3 (C,D). Dots correspond to 26 samples from three sampling stations: S1 (green), S2 (blue), S3 (red). A, B, C indicate replicates; 1: 0-2 cm; 2: 2-10 cm; 3: > 10 cm.

Among these compounds, dieldrin was the only one to show values close to or slightly higher than the ERL (2 ng g^{-1}) for about half of the samples at S2 (Table 1). This pesticide was used extensively in agriculture as an alternative to DDT until its use was forbidden by the French government in 1972. Measured HCB concentrations (up to 5.7 ng g^{-1}) were under the no-effect concentration value of 20 ng g^{-1} for chronic exposure of benthic organisms (OSPAR ERL value) (Long et al. 1995). However, the quality of the sediment could be poor (class 3) according to the environmental quality classification of sediment in Norway (Bakke et al., 2010). Following this classification, considering the sum of DDT, the sediments would be considered as good (class 2) or even, for some samples, as background (class 1) (Long et al., 1995). The maximum value of the sum of PCBs (6.8 ng g^{-1}; Table 1) was far from the sediment ERL guideline value of 23 ng g^{-1} (Long et al., 1995). The maximum value of the sum of PCBs (6.8 ng g^{-1}; Table 1) was far from the sediment ERL guideline value of 23 ng g^{-1} (Long et al., 1995). By contrast, compared to the other two stations, S3 was characterized by elevated concentrations of naphthalene (96.4 to 468.9 ng g^{-1}; Table 1), one of the 16 PAHs considered to be priority pollutants by the EPA (Bojes and Pope, 2007). According to the values of the Flt/(Flt + Pyr) ratio, usually used to discriminate the sources of PAHs, hydrocarbons detected in Cayenne River sediments are from diesel and wood combustion (Pereira et al., 2019; Pichler et al., 2021). When present in the sediments, naphthalene levels were always higher than the NOAA threshold effect level (34.57 ng g^{-1}), and for some samples, were above the NOAA ERL value (160 ng g^{-1}) (MacDonald et al., 2000).

The study of Michelet et al. (2021) on the same cores showed low averaged concentrations of the sum of the different organic contaminants measured (PAHs, organochlorine pesticides) in the whole sedimentary cores that were under the regulatory

thresholds. By considering the mean individual concentrations of compounds at each depth layers (0-2 cm; 2-10 cm; > 10 cm), it clearly appears however that some compounds were above the regulatory thresholds in some layers at stations 2 et 3 (i.e. dieldrin and naphthalene, respectively).

3.2. Prokaryotic community of mangrove sediments of Cayenne estuary

3.2.1. Estimations of community size

The total DNA extracted from the sediments (the molecular microbial biomass) was used to estimate the size of the microbial pool at the sampling stations (Dequiedt et al., 2011; Terrat et al., 2012). This proxy includes the prokaryotic communities and micro eukaryotic inhabitants of mangrove sediments (e.g., fungi and meiofauna). At stations 1 and 3, molecular microbial biomass was 3.1 ± 0.4 µg g^{-1} d.w. and 3.98 ± 0.52 g^{-1} d.w., respectively (Supplementary Data C). Higher values were observed in the surface layer at station 2 ($p = 0.05$; 7.3 ± 0.8 µg g^{-1} d.w). These molecular microbial biomass values correspond well to values reported in other mangrove sediments (~11-20 µg g^{-1}) (Fernandes et al., 2014; Jiang et al., 2011).

Within the microbial communities, differences were only observed in the size of the bacterial populations in the surface layer ($p < 0.001$). Indeed, the number of bacterial 16S rRNA gene copies was higher at station 1 than at stations 2 and 3 ($p < 0.01$) on the surface and reached 7.9×10^9 copies g^{-1} d.w. vs. 1.4×10^9 and 4.9×10^5 copies g^{-1} d.w., respectively (Supplementary Data C). The environmental conditions at station 1 and, notably, the higher OM content (1.5- to 4-fold more than other stations). seemed to promote bacterial growth (TC and TN $r_s = 0.7$, $p < 0.01$) (Kaiser and Guggenberger, 2003; Rocha et al., 2016). By contrast, the archaeal abundance was not significantly different between the three stations at any depth ($p > 0.05$; 5.8×10^6 copies g^{-1} sediment d.w.; Supplementary Data C) and corresponded to values earlier observed for other mangrove sediments (Li et al., 2019; Zhou et al., 2017).

3.2.2. Structure and composition of mangrove microbiota

After the filtering and trimming processes, 7759 ASVs were assigned (465 ± 167 ASVs by sample; Supplementary Data C), and 650 ASVs that were not assigned, representing 0.6% of the community, were removed. There was no significant difference in alpha diversity between stations ($p > 0.05$); specific richness and Shannon index fluctuated between 220 and 817 ASVs and 5.1 to 6.3, respectively (Supplementary Data C). By contrast to the soil microbiomes in Brazilian mangroves, microbiota associated with the Cayenne estuary's mangroves seems less diverse (Tavares et al., 2021).

The taxonomic composition of the mangrove microbiota encompassed 50 phyla (Supplementary Data D). These communities were predominantly composed of members of Proteobacteria (40-58%), Chloroflexi (9.0-22.3%), Acidobacteria (4.7-13.1%), Bacteroidetes (3.5-13.1%), Planctomycetes (3.7-6.9%), Crenarchaeota (1.0-9.4%), Thaumarchaeota (0.7-4.7%), Gemmatimonadetes (2.3-4.7%), and Nitrospirae (0.65-3.6%) (Figure 3). The observed prevalence of the most abundant phyla (> 3% of relative abundance) is in accordance with the literature (Andreote et al., 2012; Huergo et al., 2018; Tavares et al., 2021) suggesting that Proteobacteria, Chloroflexi, Acidobacteria, Bacteroidetes, and Planctomycetes constitute the core microbiome of mangrove sediments in the AEP region. Differences in community composition were observed between depths and stations (PERMANOVA, $p < 0.05$). At the phylum level, the heatmap clustering analysis highlighted several microbial patterns (Figure 3). In the surface mangrove sediment of the three stations, the relative abundance of the major phyla Proteobacteria, Bacteroidetes, Epsilonbacteraeota, and Kiritimatiellaeota was higher. Bacteroidetes and Kiritimatiellaeota are regarded as specialists in the degradation of macromolecules, such as complex polysaccharides and proteins, to obtain carbon, amino acids, and sulfur (McBride, 2014; Sackett et al., 2019). Both phyla could have a pivotal role in initiating the mineralization of high-molecular-weight organic matter in mangrove sediments. Within the Proteobacteria, Desulfobacteraceae (1.1-6.4%), Desulfobulbaceae (1.8-4.4%), and

Desulfarculaceae (0.4-2.2%) were dominant (Supplementary Data E). These three families are strictly anaerobic and chemoorganoheterotrophic, and they belong to the group of sulfate-reducing bacteria (Kuever, 2014). They are commonly observed in mangroves (Huergo et al., 2018; Gong et al., 2019). Mangrove sediments contain high levels of OM and sulfates, and frequently experience anaerobic conditions (Correia and Guimarães, 2017), creating favorable conditions for sulfate reduction (Gros et al., 2018; Fernández-Cadena et al., 2020). Within the Epsilonbacteraeota, sulfur-oxidizing bacteria *Sulfurimonas* (Thiovulaceae) and *Sulfurovum* (Sulfurovaceae) were the most abundant. These aerobic bacteria oxidize the sulfide produced by anaerobic sulfate-reducing bacteria, suggesting transitions between oxic and anoxic conditions in the surface sediment, probably related to tidal cycles and benthic infaunal activities. Changes of the prokaryotic communities were observed between the surficial sediment and the other sedimentary layers. Amongst the most abundant phyla, Planctomycetes and Calditrichaeota were found to be enriched in deeper sediments at S1 and S2 (Figure 3 and Supplementary Data D). Moreover, a significant increase in the relative abundance of Crenarchaeota and Gemmatimonadetes was observed at S1 and S2, respectively. Planctomycetes phylum comprises members related to Planctomycetia and Phycisphaerae, but surprisingly no known anaerobic ammonia-oxidizing microorganisms belonging to "*Candidatus* Brocardiales*"* were observed. Calditrichaeota was mostly represented by the genus *Calorithrix*, but the genus *Caldithrix* is specifically observed in deeper sediments at S1 and S2. The cultured Calditrichaeota are anaerobic, chemoorganoheterotroph, and are able to degrade detrital proteins through the use of extracellular peptidases (Marshall et al., 2017). Members of the phylum Gemmatimonadetes are characteristically detected in the soil and mangrove microbiomes (Takayasu et al., 2019; Zhang et al., 2019). Despite their widespread distribution, their physiology and ecology are poorly described (Zeng, et al., 2021). Finally, a strong vertical stratification was observed for

Crenarchaeota at S1 with higher relative abundances in the deeper sediments than in surficial sediments. Identified members of Crenarchaeota belong exclusively to Bathyarchaeota, a taxon of global generalists that are widespread in anoxic sediments (Zhou et al., 2018). Sediment depth is known to be one of the determinants in the structuration of the archaeal communities in mangrove sediment, principally due to the biogeochemical zonation along with depth profile (Zhou et al., 2017). Crenarchaeota and Lokiarchaeota usually dominate the archaeal communities in subsurface sediments, while Thaumarchaeota and Euryarchaeota dominate in surface sediments.

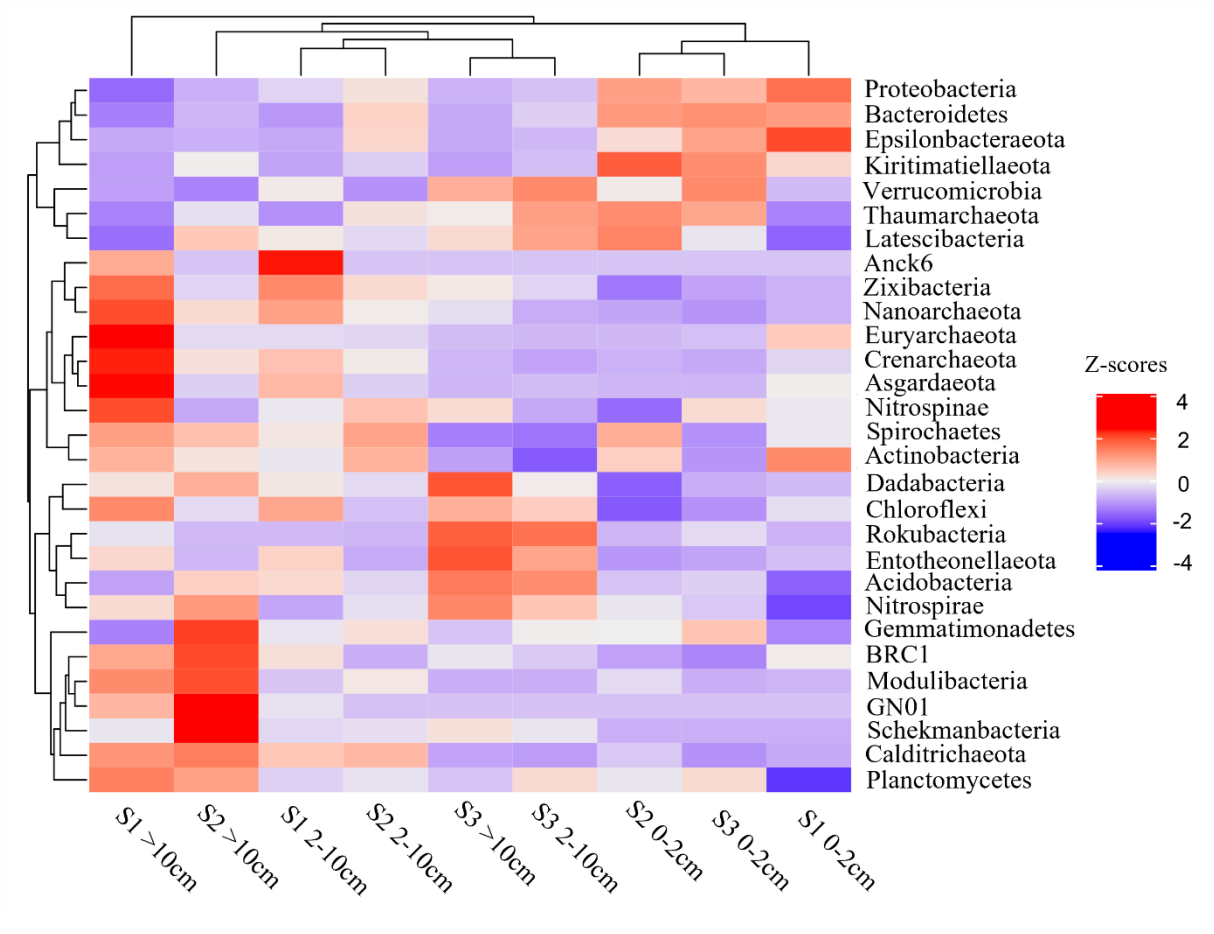

Figure 3. Z-score heatmap of top 30 phyla (representing 94.3% of total community) at three sampling stations (S1, S2, S3). Red indicates higher Z-scores (higher relative abundance compared to mean of abundance of that phylum) and blue indicates lower Z-scores (lower relative abundance).

A different trend in the vertical stratification of the microbial communities was observed at S3. In this station, Nitrospirae, Acidobacteria, and Chloroflexi were found to be enriched in the subsurface layers. Within the phylum Nitrospirae, *Nitrospira* and *Thermodesulfovibrio* were particularly abundant at S3. *Nitrospira* plays a pivotal role in the second step of nitrification as nitrite-oxidizing bacteria (NOB) in diverse natural ecosystems (Daebeler et al., 2014) or in wastewater treatment plants (Daims et al., 2011). They are often associated with ammonia oxidizing archaea (AOA) for the two-step process of nitrification. *Nitrospira* members seem also to be able to achieve complete ammonia oxidation (comammox; Daims et al., 2015). This genus is adapted to oligotrophic conditions (Daims and Wagner, 2018; Koch et al., 2019) but little is known about potential factors driving niche specialization between comammox and canonical ammonia oxidizers. *Thermodesulfovibrio* representatives occur in anaerobic environments, where they contribute to the degradation of organic compounds and indirectly to the production of methane (Daims, 2014). Among the less abundant phyla, Latescibacteria (family Latescibacteriaceae), Entotheonellaeota (family Entotheonellaceae) Dadabacteria (order Dadabacteriales), Rokubacteria (order Rokubectiales) were also more abundant in the deepest layer at S3 (Figure 3; Supplementary Data D).

Some studies have shown that factors such as pH, TC, TN, and granulometry could modulate the observed microbial patterns in mangrove sediments (Colares and Melo, 2013; Zhang et al., 2019; Li et al., 2021). The complex distributions that can be observed are notably the results of the microbial lifestyles (*e.g.*, heterotroph or oligotroph, anaerobe or aerobe) with respect to the local environmental conditions.

3.2.3. Drivers of mangrove microbiota in the Cayenne estuary

Differences in microbial community composition among the sediment samples were found to have significant correlations with four environmental factors (granulometry, dieldrin,

pH, and TC), together explaining R^2adj = 31.2%: sand percentage ($p < 0.01$, $R^2adj = 0.12$), dieldrin ($p < 0.01$, $R^2adj = 0.11$), pH ($p < 0.01$, $R^2adj = 0.04$), and TC ($p < 0.01$, $R^2adj = 0.04$).

Several studies reported the effects of clay, sand, and silt contents on the microbial communities in soils (e.g., Dequiedt et al., 2011) and mangrove sediments (Colares and Melo, 2013). Sessitsch et al. (2001) studied the effect of soil particle size fractions on microbial population structures. These authors demonstrated that the microbial structure was significantly affected by particle size, with higher diversity observed for microbiota inhabiting soil composed of smaller size fractions. The authors hypothesized that the low nutrient availability, protozoan grazing, and competition with microbes (i.e., fungi) could explain the reduced diversity in larger size fractions. Colares and Melo (2003) studied the relationship between microbial community structure and environmental factors in Brazilian mangrove sediments. Their redundancy analysis revealed that the silt–clay percentage was the most important factor controlling the microbial profiles. Particle size fractions (sand, silt, and clay) differ in mineralogical composition (Acosta at al., 2011). They have specific surface reactivity yielding the formation of organomineral complexes with different concentration, composition, and availability of associated OM (Christensen, 2001). As a consequence, these fractions represent various microenvironments in terms of organic substrates, but also oxygenation, accessible water, and nutrients, promoting the development of specific communities.

An unexpected outcome in this study was the identification of dieldrin as one of the main drivers of the distribution of microbial communities in the Cayenne estuary. To date, studies showing a shift in microbial communities as a result of organochlorine pesticides are scarce (Sangwan et al., 2012; Tejada et al., 2015; Wu et al., 2018). The effect of dieldrin on microbial communities was observed in the gastrointestinal system of zebrafish (Hua et al.,

2020), with an increased abundance of members belonging to Verrucomicrobia and a decrease in Clostridia and Betaproteobacteria. Organochlorines can also induce shifts in microbial functions in soils, such as through suppression of nitrogen-fixing bacteria that have a pivotal role in replenishing natural nitrogen fertilizer in soil (Poltera, 2007).

In biogeography studies, pH was recognized as another factor determining the microbiota structure of soils in terms of richness, diversity, and composition (Fierer and Jackson, 2007; Lauber et al., 2009; Dequiedt et al 2011). Chen et al. (2016) and Li et al. (2021) showed that in mangroves, pH is also one of the main factors explaining the microbial community composition in sediments regardless of the season or developmental stage of the mangrove forest. pH was also shown to be the best predictor of community structure and the relative abundance of major dominant lineages at the continental scale in North and South America (Lauber et al., 2009). Most microorganisms have a low tolerance to pH variations that affect biogeochemical processes and their activities and related biogeochemical processes (Nicol et al., 2008).

Other studies have shown that mangrove microbiota composition responds strongly to other physicochemical properties of the sediment, such as TC content (Colares and Melo, 2003; Zhang et al 2019; Li et al., 2021). Colares and Melo (2003) highlighted a significant correlation between microbial community structure and OM content in Brazilian mangroves. Zhang et al. (2019) characterized the microbiota from six Chinese mangroves and showed that mean annual precipitation and TC were the main factors explaining the distribution of the community. Tidal cycles (Zhang et al., 2018) and variables associated with the vegetation above (e.g., Jiang, et al., 2013; Gomes et al., 2014, Luis et al., 2019) have also been reported to be drivers of the distribution and structure of bacterial communities of mangrove soils and sediments.

3.3. Potential microbial bioindicators of anthropogenic pressures

Potential microbial bioindicators of anthropogenic pressure were found based on the correlations between specific taxa and the variables associated with the three types of anthropogenic pressure identified along the urban-to-rural gradient of the Cayenne estuary (OM enrichment and organochlorine and naphthalene contamination).

3.3.1. Microbial signature of slight OM enrichment in mangrove

Several microbial taxa exhibited a negative or positive correlation with OM enrichment (TC), making them serious candidates for bioindication purposes (Figure 4).

This is the case of the Bathyarchaeota class, formerly known as the Miscellaneous Crenarchaeotal Group (MCG), (0.93-8.1%), which was positively correlated with TC ($r_s = 0.6$, $p < 0.01$; Figure 4A, Supplementary Data F). In mangrove sediments, Bathyarchaeota is the dominant archaeal taxon (Zhou et al., 2017, 2018), its abundance was suggested to be mainly correlated with total organic carbon content (Xiang et al., 2017; Yu et al., 2017). This observation may be associated with their heterotrophic lifestyle and their ability to anaerobically use detrital proteins, fatty acids/aromatic compounds, polymeric carbohydrates, and other OM (Lazar et al., 2016; Meng et al., 2014). Despite the diversity of Bathyarchaeota (over 25 subgroups) (Zhou et al., 2018) and their environmental preferences, the abundance of the overall population seems to be a good indicator of OM enrichment in mangrove.

The levels of Euryarchaeota (0-1.6%) and Asgardaeota (0-0.88%), both highly abundant in anaerobic marine sediments (Hoshino et al., 2020), were also correlated with TC (both $r_s = 0.7$, $p < 0.01$; Figure 4A). Almost all the ASVs in the phylum Euryarchaeota were included in the Thermoplasmata sublineage, especially in the anaerobic heterotrophic MBG-D archaeal group (newly named Thermoprofundales). In recent years, single-cell genomic and metagenomic approaches have shown that MBG-D archaea are capable of exogenous protein mineralization and acetogenesis in marine sediment (Lazar et al., 2017; Lloyd et al., 2013). In

mangrove sediments, these archaea appear to be capable of transporting and assimilating peptides and generating acetate and ethanol through fermentation (Zhou et al., 2019). In the phylum Asgardaeota, the majority of ASVs belong to Lokiarchaeota, which vary in their metabolic activity, and their in situ activities are still largely unknown (Yin et al., 2021).

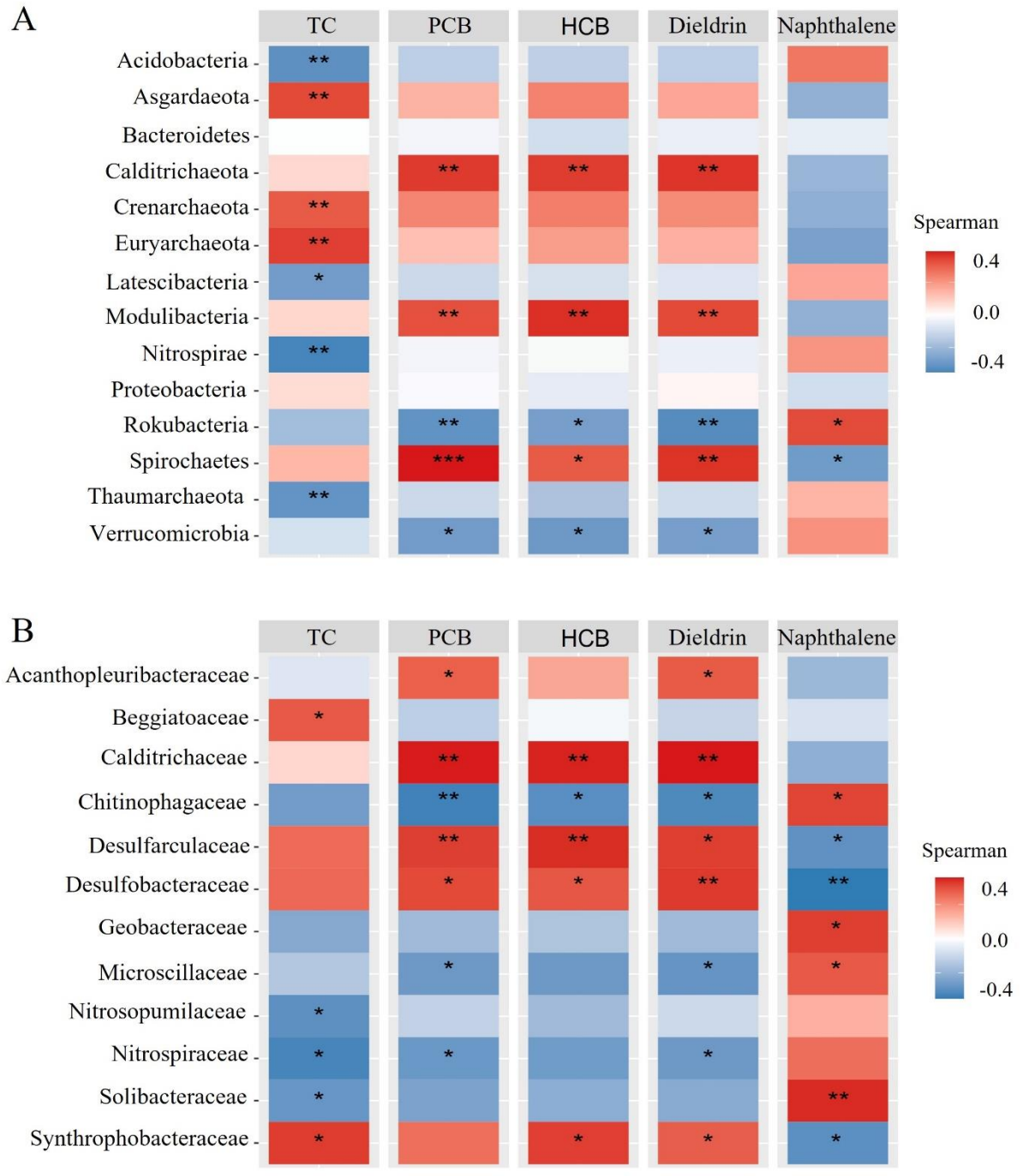

Spearman's rank correlation coefficient heatmap showing relationships between environmental variables and interesting taxa. A: phylum level; B: family level. Statistically significant Spearman correlations are highlighted (*p < 0.05, **p < 0.01, ***p < 0.001).

By contrast, Nitrospirae (r_s = −0.7; $p < 0.01$), Acidobacteria (r_s = −0.6; $p < 0.01$), Thaumarchaeota (r_s = −0.6; $p < 0.01$), and Latescibacteria (r_s = −0.6; $p < 0.01$) were negatively correlated with TC (Figure 4A). The majority of Thaumarchaeota ASVs (38 ASVs) belong to "*Candidatus* Nitrosopumilus", which are mesophilic, autotrophic, and aerobic AOA. Some groups of Thaumarchaeota are recognized as major contributors of ammonia oxidation (the first step in nitrification) in marine oligotrophic ecosystems (Pester et al., 2011; Wang et al., 2019) and could be dominant in some ecosystems, such as in the Amazon River and its plume (Pinto et al., 2020). Ammonia oxidation is known to be inhibited by several parameters, notably organic carbon content (Pester et al., 2012), OM quality (Strauss and Lamberti, 2000), and the TC:TN ratio (Bates et al., 2011). AOA are adapted to low ammonium concentrations and are outcompeted by bacteria when concentrations become higher (Nakagawa and Stahl, 2013). Sensitivity to slight OM enrichment was also observed for the *Nitrospira* genus (19 ASVs; 0-0.9%; r_s = −0.68; $p < 0.05$), the NOB and comammox bacteria. Latescibacteria (formerly WS3) represents a ubiquitous phylum found in terrestrial, aquatic, and marine environments (Youssef et al., 2015). Metabolic reconstruction suggests a saprophytic lifestyle for this candidate phylum, with a marked capacity for decomposition of OM (proteins, lipids, and polysaccharides) predominant in plant, bacterial, fungal, crustacean, and eukaryotic algal cell walls (Farag et al., 2017; Youssef et al., 2015). Finally, a negative correlation between Acidobacteria abundance and TC content was observed in our dataset (Figure 4A), as it was also in terrestrial ecosystems, leading to the conclusion that members of this taxon may be oligotrophic bacteria (Fierer et al., 2007).

3.3.2. Taxa sensitive to organochlorine compounds

Correlations between several microbial taxa and organochlorine (dieldrin, PCB, and HCB) concentrations were observed (Figure 4; Supplementary Data F).

582 Calditrichaeota (Calditrichaceae family) and Spirochaetes (*Spirochaeta* genus) were
583 significantly correlated ($r_s < 0.7$; $p < 0.05$) with PCB, HCB, and dieldrin content (Figure 4).
584 Spirochaetes are indigenous to sulfide-rich mud or sediments (Tanner et al., 2000; Leschine et
585 al., 2006) and are typically found in PCB-contaminated waters (Dong et al., 2018) or
586 contaminated sediments (Quero et al., 2015). Calditrichaeota and Spirochaeota are known to
587 be very diversified and to have a wide range of ecological niches (Leschine et al., 2006;
588 Marshall et al., 2017). Until now, these organisms have never been associated with
589 dechlorination of organochlorine compounds; however, our results suggest that
590 Calditrichaeota and *Spirochaeta* could have a role in the degradation of PCB, HCB, and
591 dieldrin, or at least could be tolerant to these compounds. Future experimental studies are
592 needed to validate this finding (e.g., biodegradation assays). "*Candidatus* Modulibacteria"
593 phylum (previously named KS3B3 or GN03) was also positively correlated with the three
594 organochlorine compounds. By contrast, "*Candidatus* Rokubacteria" (0–1.5%; previously
595 named SPAM or candidate division NC10) was negatively correlated with PCB ($r_s = -0.6$; $p <$
596 0.05), HCB ($r_s = -0.6$; $p < 0.001$), and dieldrin ($r_s = -0.7$; $p < 0.01$). This phylum is found in
597 diverse terrestrial ecosystems such as alpine soil, crop soil, or copper mine soil (Becraft et al
598 2017), and this is the first time that it is identified in a marine ecosystem. The lack of
599 knowledge on "*Candidatus* Modulibacteria" and "*Candidatus* Rokubacteria", two phyla
600 without cultivable representatives, does not allow us to explain the significant correlations
601 with organochlorine compounds in this study. The relative abundance of the Verrucomicrobia
602 phylum was significantly higher at S3 than at S1 and S2 (0.49%; $p < 0.05$). This taxon is
603 related to the Planctomycetes–Verrucomicrobia–Chlamydia superphylum, has diverse
604 metabolism capabilities (such as methanogenesis and degradation of sulfated polysaccharides)
605 (Freitas et al., 2012; Van Vliet et al., 2019), and is typically found in mangrove sediments
606 (Liang et al., 2007; Nogueira et al., 2015). It was negatively correlated with PCB ($r_s = -0.6$; p

607 < 0.05), HCB (r_s = −0.6; p < 0.05), and dieldrin (r_s = −0.5; p < 0.05), suggesting that
608 Verrucomicrobia is sensitive to the organochlorine compounds in mangrove sediments.
609 At the family level, some taxa seem particularly interesting in their response to PCB
610 pressure, notably in the Desulfobacterota (formerly Deltaproteobacteria) phylum. Two
611 families were significantly correlated with PCB content (Figure 4B): Desulfobacteraceae (r_s =
612 0.6; p < 0.05) and Desulfarculaceae (r_s = 0.6; p < 0.001). These Desulfobacterota are strictly
613 anaerobic and sulfate-reducing bacteria, and are indirectly implicated in PCB dechlorination
614 by promoting organohalide respiration of PCB dechlorinating bacteria (Praveckova et al.,
615 2016; Matturro et al., 2020). The Acanthopleuribacteraceae family (Acidobacteria) is known
616 to degrade PCB and is considered very useful in remediating polluted environments
617 (Falkiewicz-Dulik et al., 2015). The significant response of Acanthopleuribacteraceae (r_s =
618 0.6; p < 0.01) to the low quantity of PCBs measured makes this taxon a particularly
619 interesting bioindicator of PCB contamination.
620
621 **3.3.3. Bacterial signature of naphthalene contamination in mangrove**
622 Although naphthalene content was above the regulatory threshold, it was not identified
623 as one of the main drivers of mangrove microbiota along the estuary. However, the levels of
624 some taxa were positively correlated with naphthalene content, such as uncultured
625 Rokubacteria phylum (r_s = 0.5, p < 0.05; Fig. 4A). As seen previously, Rokubacteria are not
626 well described, but their diversified genome reveals a potential implication in the nitrogen,
627 methane, and sulfur cycles (Hug et al., 2013; Becraft et al., 2017). However, a meta-analysis
628 of the rokubacterial MAGS conducted by Kroeger et al. (2018) showed that taxa members
629 have several features involved in metabolizing long and short hydrocarbons in soil via two
630 enzymes, cytochrome P450 and alkane 1-monooxygenase, respectively. Cytochrome P450
631 has been described as one of the enzymes involved in the naphthalene biodegradation
632 (Mohapatra and Prashant, 2021) which may explain the observed positive correlation. These

details can explain the positive correlation observed in this study. Within the Acidobacteria, the Solibacteraceae family was also positively correlated with naphthalene ($r_s = 0.7$; $p < 0.01$; Figure 4B). Members of this family possess some functional genes that allow them to degrade branched hydrocarbons such as pristane (Wang et al., 2016), yet it has not been proven if they can degrade PAHs.

A correlation between the Chitinophagaceae family and naphthalene was observed ($r_s = 0.6$; $p < 0.05$). Strains of this family have been isolated from freshwater sediments and soil contaminated with petroleum (Blanco-Enríquez et al., 2018). Members of Chitinophagaceae are known to be able to degrade biopolymers (Gomes et al., 2010) and to belong to microbial consortia that remove PAHs. Specifically, some members of Chitinophagaceae have the capacity to degrade pyrene and benzo[a]pyrene in water (Blanco-Enriquez et al., 2018), but no significant correlation was found in this study between Chitinophagaceae and these two compounds, which were barely detected in the samples. No direct link between Chitinophagaceae and naphthalene degradation is reported in the literature. Similarly, Geobacteraceae, a sulfur-reducing and iron-reducing Desulfobacterota bacteria (Kleindienst et al., 2012) were positively correlated with naphthalene ($r_s = 0.6$; $p < 0.01$; Figure 4B). Some studies have shown that this family has the capacity to degrade aromatic compounds and PAHs (Coates et al., 2001; Holmes et al., 2004; Durante-Rodríguez et al., 2018), and it was used in the bioremediation of organic contaminants in the soil subsurface (Holmes et al., 2004).

4. Conclusion

Our study shows that estuarine mangroves of the Cayenne River are globally exposed to low anthropogenic pressures. However, we detected low OM enrichment, and organochlorine and pyrolytic PAH pollution derived from human activities, mainly at the stations closest to the city of Cayenne (S1 and S2). The core microbial taxa are similar to the

one observed in Brazil mangroves, which are more impacted by human activities. Granulometry, dieldrin concentration, pH, and TC content appear to drive the mangrove microbiota. Taxa of interest were identified that are correlated to OM enrichment and organochlorine (dieldrin, PCB and HCB) and naphthalene contamination, represent potential bioindicators of the health status of the mangrove ecosystem. However, much more research is needed to assess the structural, spatial, and temporal distributions of microbial communities in mangroves as well as their response to growing anthropogenic pressures in an overall still relatively preserved environment.

Data Availability Statement: The data presented in this study are openly available in https://doi. org/10.5281/zenodo.4592299 [doi:10.5281/zenodo.4592299].

Acknowledgments

This work was co-funded by the Office de l'Eau de la Guyane and by Office Français pour la Biodiversité within the framework of the project: "Study of sediment functioning in French Guiana mangroves toward the identification of bio-indicators to monitor estuarine and coastal water bodies ecological status". The project leading to this publication has received funding from the European FEDER Fund under project no. 1166-39417. We acknowledge an "Investissement d'Avenir" grant managed by the Agence Nationale de la Recherche (CEBA, ref. ANR-10-LABX-25-01). The authors thank M. Brossard (IRD-Cayenne), A. Gardel, T. Maury and S. Morvan (LEEISA-Cayenne) for providing logistic support for the in situ work. We thank J. Devesa (LEMAR) for CHN analysis and F. Fromard for constructive discussions at an early stage of the project.

685 **References**

686 Aciego Pietri, J.C., Brookes, P. C., 2008. Relationships between soil pH and microbial
687 properties in a UK arable soil. Soil Biol. and Biochem. 40, 1856–1861.
688 https://doi.org/10.1016/j.soilbio.2008.03.020
689 Acosta, J. A., Martínez-Martínez, S., Faz, A., Arocena, J., 2011. Accumulations of major and
690 trace elements in particle size fractions of soils on eight different parent materials.
691 Geoderma 161, 30–42. https://doi.org/10.1016/j.geoderma.2010.12.001
692 Alongi, D.M., 1994. The role of bacteria in nutrient recycling in tropical mangrove and other
693 coastal benthic ecosystems. Hydrobiologia 285, 19–32.
694 https://doi.org/10.1007/BF00005650
695 Andreote, F. D., Jiménez, D. J., Chaves, D., Dias, A. C. F., Luvizotto, D. M., Dini-Andreote,
696 F., Fasanella, C. C., Lopez, M. V., Baena, S., Taketani, R. G., De Melo, I. S., 2012. The
697 microbiome of Brazilian mangrove sediments as revealed by metagenomics. PLoS ONE
698 7. 38600. https://doi.org/10.1371/journal.pone.0038600
699 Anthony, E.J., Gardel, A., Gratiot, N., Proisy, C., Allison, M.A., Dolique, F., Fromard, F.,
700 2010. The Amazon-influenced muddy coast of South America: A review of mud-bank-
701 shoreline interactions. Earth-Science Rev. 103, 99–121.
702 https://doi.org/10.1016/j.earscirev.2010.09.008
703 Bakke, T., Källqvist, T., Ruus, A., Breedveld, G. D., Hylland, K., 2010. Development of
704 sediment quality criteria in Norway. JSSS. 10, 172–178.
705 https://doi.org/10.1007/s11368-009-0173-y
706 Bates, S.T., Berg-Lyons, D., Caporaso, J.G., Walters, W.A., Knight, R., Fierer, N., 2011.
707 Examining the global distribution of dominant archaeal populations in soil. ISME J. 5,
708 908–917. https://doi.org/10.1038/ismej.2010.171
709 Becraft, E.D., Woyke, T., Jarett, J., Ivanova, N., Godoy-Vitorino, F., Poulton, N., Brown,

J.M., Brown, J., Lau, M.C.Y., Onstott, T., Eisen, J.A., Moser, D., Stepanauskas, R., 2017. Rokubacteria: Genomic giants among the uncultured bacterial phyla. Front. Microbiol. 8, 1–12. https://doi.org/10.3389/fmicb.2017.02264

Blanco-Enríquez, E.G., De La Serna, F.J.Z.D., Peralta-Pérez, M.D.R., Ballinas-Casarrubias, L., Salmerón, I., Rubio-Arias, H., Rocha-Gutiérrez, B.A., 2018. Characterization of a microbial consortium for the bioremoval of polycyclic aromatic hydrocarbons (PAHs) in water. Int. J. Environ. Res. Public Health 15. https://doi.org/10.3390/ijerph15050975

Bojes, H.K., Pope, P.G., 2007. Characterization of EPA's 16 priority pollutant polycyclic aromatic hydrocarbons (PAHs) in tank bottom solids and associated contaminated soils at oil exploration and production sites in Texas. Regul. Toxicol. Pharmacol. 47, 288–295. https://doi.org/10.1016/j.yrtph.2006.11.007

Brändli, R.C., Bucheli, T.D., Kupper, T., Mayer, J., Stadelmann, F.X., Tarradellas, J., 2007. Fate of PCBs, PAHs and their source characteristic ratios during composting and digestion of source-separated organic waste in full-scale plants. Environ. Pollut. 148, 520–528. https://doi.org/10.1016/j.envpol.2006.11.021

Bunting, P., Rosenqvist, A., Lucas, R., Rebelo, L.-M., Hilarides, L., Thomas, N., Hardy, A., Itoh, T., Shimada, M., Finlayson, C., 2018. The global mangrove watch - A new 2010 global baseline of mangrove extent. Remote Sens. 10, 1669. https://doi.org/10.3390/rs10101669

Burton, G.A., 2002. Sediment quality criteria in use around the world. Limnology 3, 65–75. https://doi.org/10.1007/s102010200008

Callahan, B.J., McMurdie, P.J., Rosen, M.J., Han, A.W., Johnson, A.J.A., Holmes, S.P., 2016. DADA2: High-resolution sample inference from Illumina amplicon data. Nat. Methods 13, 581–583. https://doi.org/10.1038/nmeth.3869

Carugati, L., Gatto, B., Rastelli, E., Lo Martire, M., Coral, C., Greco, S., Danovaro, R., 2018.

735 Impact of mangrove forests degradation on biodiversity and ecosystem functioning. Sci.
736 Rep. 8, 1–11. https://doi.org/10.1038/s41598-018-31683-0
737 Chambers, L.G., Guevara, R., Boyer, J. N., Troxler, T.G., Davis, S.E., 2016. Effects of
738 salinity and inundation on microbial community structure and function in a mangrove
739 peat soil. Wetlands 36, 361–371. https://doi.org/10.1007/s13157-016-0745-8
740 Chen, Q., Zhao, Q., Li, J., Jian, S., Ren, H.,2016. Mangrove succession enriches the sediment
741 microbial community in South China. Sci. Rep. 6, 1–9.
742 https://doi.org/10.1038/srep27468
743 Christensen, B., T., 2001. Physical fractionation of soil and structural and functional
744 complexity in organic matter turnover. Eur. J. Soil Sci., 52, 345–353.
745 https://doi.org/10.1046/j.1365-2389.2001.00417.x
746 Coates, J.B., Chakraborty, R., Lack, J.G., O'Connor, S.M., Cole, K.A., Bender, K.S.,
747 Achenbach, L.A., 2001. Anaerobic benzene oxidation coupled to nitrate reduction in
748 pure culture by two strains of Dechloromonas. Nature 411, 1039–1043.
749 https://doi.org/10.1038/35082545
750 Colares, G. B., Melo, V. M. M., 2013. Relating microbial community structure and
751 environmental variables in mangrove sediments inside Rhizophora mangle L. habitats.
752 Appl. Soil Ecol. 64, 171–177. https://doi.org/10.1016/j.apsoil.2012.12.004
753 Correia, R.R.S., Guimarães, J.R.D., 2017. Mercury methylation and sulfate reduction rates in
754 mangrove sediments, Rio de Janeiro, Brazil: The role of different microorganism
755 consortia. Chemosphere 167, 438–443.
756 https://doi.org/10.1016/j.chemosphere.2016.09.153
757 Daebeler, A., Le Bodelier, P., Yan, Z., Hefting, M.M., Jia, Z., Laanbroek, H.J., 2014.
758 Interactions between Thaumarchaea, Nitrospira and methanotrophs modulate autotrophic
759 nitrification in volcanic grassland soil. ISME J. 8, 2397–2410.

https://doi.org/10.1038/ismej.2014.81

Daims, H., Lücker, S., LePaslier, D., Wagner, M., 2011. Diversity, environmental genomics, and ecophysiology of nitrite-oxidizing bacteria. In Nitrification. Ward, B.B., Arp, D.J., Klotz, M.G. (eds). Washington, DC, USA: ASM Press, pp. 295–322. https://doi.org/10.1128/9781555817145.ch12

Daims H., 2014. The Family Nitrospiraceae. In: Rosenberg E., DeLong E.F., Lory S., Stackebrandt E., Thompson F. (eds) The Prokaryotes. Springer, Berlin, Heidelberg. https://doi.org/10.1007/978-3-642-38954-2_126

Daims, H., Lebedeva, E. V., Pjevac, P., Han, P., Herbold, C., Albertsen, M., Jehmlich, N., Palatinszky, M., Vierheilig, J., Bulaev, A., Kirkegaard, R.H., Von Bergen, M., Rattei, T., Bendinger, B., Nielsen, P.H., Wagner, M., 2015. Complete nitrification by Nitrospira bacteria. Nature 528, 504–509. https://doi.org/10.1038/nature16461

Daims, H., Wagner, M., 2018. Nitrospira. Trends Microbiol. 26, 462-463. https://doi.org/10.1016/j.tim.2018.02.001

DeAngelis, K. M., Silver, W. L., Thompson, A. W., & Firestone, M. K., 2010. Microbial communities acclimate to recurring changes in soil redox potential status. Environ. Microbiol., 12, 3137–3149. https://doi.org/10.1111/j.1462-2920.2010.02286.x

Dequiedt, S., Saby, N.P.A., Lelievre, M., Jolivet, C., Thioulouse, J., Toutain, B., Arrouays, D., Bispo, A., Lemanceau, P., Ranjard, L., 2011. Biogeographical patterns of soil molecular microbial biomass as influenced by soil characteristics and management: Biogeography of soil microbial biomass. Glob. Ecol. Biogeogr. 20, 641–652. https://doi.org/10.1111/j.1466-8238.2010.00628.x

Dias, A.C.F., Andreote, F.D., Rigonato, J., Fiore, M.F., Melo, I.S., Araújo, W.L., 2010. The bacterial diversity in a Brazilian non-disturbed mangrove sediment. Antonie van Leeuwenhoek, Int. J. Gen. Mol. Microbiol. 98, 541–551.

https://doi.org/10.1007/s10482-010-9471-z

Dias, A.C.F., Dini-Andreote, F., Taketani, R.G., Tsai, S.M., Azevedo, J.L., de Melo, I.S., Andreote, F.D., 2011. Archaeal communities in the sediments of three contrasting mangroves. J. Soils Sediments 11, 1466–1476. https://doi.org/10.1007/s11368-011-0423-7

Diop, B., Sanz, N., Blanchard, F., Walcker, R., Gardel, A., 2016. The role of mangrove in the French Guiana shrimp fishery. J. Environ. Econ. Policy 8, 147–158. https://doi.org/10.1080/21606544.2018.1522601

Donato, D.C., Kauffman, J.B., Murdiyarso, D., Kurnianto, S., Stidham, M., Kanninen, M., 2011. Mangroves among the most carbon-rich forests in the tropics. Nat. Geosci. 4, 293–297. https://doi.org/10.1038/ngeo1123

Dong, X., Greening, C., Brüls, T., Conrad, R., Guo, K., Blaskowski, S., Kaschani, F., Kaiser, M., Laban, N.A., Meckenstock, R.U., 2018. Fermentative Spirochaetes mediate necromass recycling in anoxic hydrocarbon-contaminated habitats. ISME J. 12, 2039–2050. https://doi.org/10.1038/s41396-018-0148-3

Duke, N.C., 1992. Mangrove floristics and biogeography. Coast. Estuar. Stud. 41, 63–100. https://doi.org/10.1029/ce041p0063

Durante-Rodríguez, G., Gómez-Álvarez, H., Blázquez, B., Fernández-Llamosas, H., Martín-Moldes, Z., Sanz, D., Nogales, J., Carmona, M., Díaz, E., 2018. Anaerobic pathways for the catabolism of aromatic compounds. Great Britain: Royal Society of Chemistry. pp. 333–90. https://doi.org/10.1039/9781788010351-00333

Escofier, B., Pagès, J., 1994. Multiple factor analysis (AFMULT package). Comput. Stat. Data Anal. 18, 121–140. https://doi.org/10.1016/0167-9473(94)90135-X

European Union (2013) Directive 2013/39/EU of the European Parliament and of the Council amending Directives 2000/60/EC and 2008/105/EC as regards priority substances in the

field of water policy. Off J Eur Union L 226:1–17, 24 Sep 2013

Falkiewicz-Dulik, M., Janda, K., Wypych, G., 2015. Microorganism involved in biodegradation of materials. In Handbook of material biodegradation, biodeterioration and biostablization, 2nd ed., Chemtec Publishing, Toronto pp. 190. https://doi.org/10.1016/b978-1-895198-87-4.50004-9

Farag, I.F., Youssef, N.H., Elshahed, M.S., 2017. Global distribution patterns and pangenomic diversity of the candidate phylum "Latescibacteria" (WS3). Appl. Environ. Microbiol.83, 517-521. https://doi.org/10.1128/AEM.00521-17

Fernandes, S.O., Kirchman, D.L., Michotey, V.D., Bonin, P.C., Lokabharathi, P.A., 2014. Bacterial diversity in relatively pristine and anthropogenically-influenced mangrove ecosystems (Goa, India). Brazilian J. Microbiol. 45, 1161–1171. https://doi.org/10.1590/S1517-83822014000400006

Fernández-Cadena, J.C., Ruíz-Fernández, P.S., Fernández-Ronquillo, T.E., Díez, B., Trefault, N., Andrade, S., la Iglesia, R., 2020. Detection of sentinel bacteria in mangrove sediments contaminated with heavy metals. Mar. Pollut. Bull. 150, 110701. https://doi.org/10.1016/j.marpolbul.2019.110701

Fierer, N., Bradford, M.A., Jackson, R.B., 2007. Toward an ecological classification of soil bacteria. Ecology 88, 1354–1364. https://doi.org/10.1890/05-1839

Freitas, S., Hatosy, S., Fuhrman, J.A., Huse, S.M., Mark Welch, D.B., Sogin, M.L., Martiny, A.C., 2012. Global distribution and diversity of marine Verrucomicrobia. ISME J. 6, 1499–1505. https://doi.org/10.1038/ismej.2012.3

Fromard, F., Vega, C., Proisy, C., 2004. Half a century of dynamic coastal change affecting mangrove shorelines of French Guiana. A case study based on remote sensing data analyses and field surveys. Mar. Geol., 208, 265–280. https://doi.org/10.1016/j.margeo.2004.04.018

Gomes, N.C.M., Cleary, D.F.R., Pinto, F.N., Egas, C., Almeida, A., Cunha, A., Mendonça-Hagler, L.C.S., Smalla, K., 2010. Taking root: Enduring effect of rhizosphere bacterial colonization in mangroves. PLoS One 5, 1–10. https://doi.org/10.1371/journal.pone.0014065

Gomes, N.C.M., Cleary, D.F.R., Pires, A.C.C., Almeida, A., Cunha, A., Mendonça-Hagler, L.C.S., Smalla, K., 2014. Assessing variation in bacterial composition between the rhizospheres of two mangrove tree species. Estuar. Coast. Shelf Sci. 139, 40–45. https://doi.org/10.1016/j.ecss.2013.12.022

Gong, B., Cao, H., Peng, C., Perčulija, V., Tong, G., Fang, H., Wei, X., Ouyang, S., 2019. High-throughput sequencing and analysis of microbial communities in the mangrove swamps along the coast of Beibu Gulf in Guangxi, China. Sci. Rep., 9, 1–10. https://doi.org/10.1038/s41598-019-45804-w

Gordon, E.S., Goni, M.A., 2003. Sources and distribution of terrigenous organic matter delivered by the Atchafalaya River to sediments in the northern Gulf of Mexico. Geochim. Cosmochim. Acta 67, 2359–2375. https://doi.org/10.1016/S0016-7037(02)01412-6

Gros, O., Bisqué, L., Sadjan, M., Azede, C., Jean-Louis, P., Guidi-Rontani, C., 2018. First description of a new uncultured purple sulfur bacterium colonizing marine mangrove sediment in the Caribbean: Halochromatium-like PSB from Guadeloupe. Comptes Rendus - Biol. 341, 387–397. https://doi.org/10.1016/j.crvi.2018.07.001

Gu, Z., Eils, R., Schlesner, M., 2016. Complex heatmaps reveal patterns and correlations in multidimensional genomic data. J. Bioinform. 32, 2847–2849. https://doi.org/10.1093/bioinformatics/btw31

Holmes, D.E., Nevin, K.P., Lovley, D.R., 2004. In Situ Expression of nifD in Geobacteraceae in Subsurface Sediments. Appl. Environ. Microbiol. 70, 7251–7259.

https://doi.org/10.1128/AEM.70.12.7251-7259.2004

Hoshino, T., Doi, H., Uramoto, G.I., Wörmer, L., Adhikari, R.R., Xiao, N., Morono, Y., D'Hondt, S., Hinrichs, K.U., Inagaki, F., 2020. Global diversity of microbial communities in marine sediment. Proc. Natl. Acad. Sci. U. S. A. 117, 27587–27597. https://doi.org/10.1073/pnas.1919139117

Hua, Q., Adamovsky, O., Vespalcova, H., Boyda, J., Schmidt, J. T., Kozuch, M., Craft, S. L. M., Ginn, P. E., Smatana, S., Budinska, E., Persico, M., Bisesi, J. H., Martyniuk, C. J. 2021. Microbiome analysis and predicted relative metabolomic turnover suggest bacterial heme and selenium metabolism are altered in the gastrointestinal system of zebrafish (Danio rerio) exposed to the organochlorine dieldrin. Environ. Pollut. 268, 115715. https://doi.org/10.1016/j.envpol.2020.115715

Huergo, L. F., Rissi, D. V., Elias, A. S., Gonçalves, M. V., Gernet, M. V., Barreto, F., Dahmer, G. W., Reis, R. A., Pedrosa, F. O., Souza, E. M., Monteiro, R. A., Baura, V. A., Balsanelli, E., Cruz, L. M., 2018. Influence of ancient anthropogenic activities on the mangrove soil microbiome. Sci. Total Environ., 645, 1–9. https://doi.org/10.1016/j.scitotenv.2018.07.094

Hug, L.A., Castelle, C.J., Wrighton, K.C., Thomas, B.C., Sharon, I., Frischkorn, K.R., Williams, K.H., Tringe, S.G., Banfield, J.F., 2013. Community genomic analyses constrain the distribution of metabolic traits across the Chloroflexi phylum and indicate roles in sediment carbon cycling. Microbiome 1, 1. https://doi.org/10.1186/2049-2618-1-22

Jiang, Y.X., Wu, J.G., Yu, K.Q., Ai, C.X., Zou, F., Zhou, H.W., 2011. Integrated lysis procedures reduce extraction biases of microbial DNA from mangrove sediment. J. Biosci. Bioeng. 111, 153–157. https://doi.org/10.1016/j.jbiosc.2010.10.006

Jiang, X.T., Peng, X., Deng, G.H., Sheng, H.F., Wang, Y., Zhou, H.W., Tam, N.F.Y., 2013.

Illumina Sequencing of 16S rRNA Tag Revealed Spatial Variations of Bacterial Communities in a Mangrove Wetland. Microb. Ecol. 66, 96–104. https://doi.org/10.1007/s00248-013-0238-8

Kaiser, K., Guggenberger, G., 2003. Mineral surfaces and soil organic matter. Eur. J. Soil Sci. 54, 219–236. https://doi.org/10.1046/j.1365-2389.2003.00544.x

Kassambara, A. and Mundt, F., 2020. Factoextra: extract and visualize the results of multivariate data analyses. R package version 1.0.7. https://cran.r-project.org/web/packages/factoextra/index.html

Katsoyiannis, A., Terzi, E., Cai, Q.Y., 2007. On the use of PAH molecular diagnostic ratios in sewage sludge for the understanding of the PAH sources. Is this use appropriate? Chemosphere 69, 1337–1339. https://doi.org/10.1016/j.chemosphere.2007.05.084

Kleindienst, S., Ramette, A., Amann, R., Knittel, K., 2012. Distribution and in situ abundance of sulfate-reducing bacteria in diverse marine hydrocarbon seep sediments: Sulfate-reducing bacteria at marine hydrocarbon seeps. Environ. Microbiol. 14, 2689–2710. https://doi.org/10.1111/j.1462-2920.2012.02832.x

Klindworth, A., Pruesse, E., Schweer, T., Peplies, J., Quast, C., Horn, M., Glöckner, F.O., 2013. Evaluation of general 16S ribosomal RNA gene PCR primers for classical and next-generation sequencing-based diversity studies. Nucleic Acids Res. 41, 1–11. https://doi.org/10.1093/nar/gks808

Koch, H., van Kessel, M.A.H.J., Lücker, S., 2019. Complete nitrification: insights into the ecophysiology of comammox Nitrospira. Appl. Microbiol. Biotechnol. https://doi.org/10.1007/s00253-018-9486-3

Kroeger, M.E., Delmont, T.O., Eren, A.M., Meyer, K.M., Guo, J., Khan, K., Rodrigues, J.L.M., Bohannan, B.J.M., Tringe, S.G., Borges, C.D., Tiedje, J.M., Tsai, S.M., Nüsslein, K., 2018. New biological insights into how deforestation in amazonia affects

soil microbial communities using metagenomics and metagenome-assembled genomes. Front. Microbiol. 9, 1635. https://doi.org/10.3389/fmicb.2018.01635

Kuever, J., 2014. The Family Desulfarculaceae, in: Rosenberg, E., DeLong, E.F., Lory, S., Stackebrandt, E., Thompson, F. (Eds.), The Prokaryotes. Springer Berlin Heidelberg, Berlin, Heidelberg, pp. 41–44. https://doi.org/10.1007/978-3-642-39044-9_270

Laffoley, D., Grimsditch, G.D., 2009. The Management of Natural Coastal Carbon Sinks. IUCN.

Lauber, C. L., Hamady, M., Knight, R., Fierer, N., 2009. Pyrosequencing-based assessment of soil pH as a predictor of soil bacterial community structure at the continental scale. Appl. Environ. Microbiol., 75, 5111–5120. https://doi.org/10.1128/AEM.00335-09

Lazar, C.S., Baker, B.J., Seitz, K., Hyde, A.S., Dick, G.J., Hinrichs, K.-U., Teske, A.P., 2016. Genomic evidence for distinct carbon substrate preferences and ecological niches of Bathyarchaeota in estuarine sediments: Genomic content of uncultured benthic Bathyarchaeota. Environ. Microbiol. 18, 1200–1211. https://doi.org/10.1111/1462-2920.13142

Lazar, C.S., Baker, B.J., Seitz, K.W., Teske, A.P., 2017. Genomic reconstruction of multiple lineages of uncultured benthic archaea suggests distinct biogeochemical roles and ecological niches. ISME J. 11, 1118–1129. https://doi.org/10.1038/ismej.2016.189

Lê, S., Josse, J., Husson, F., 2008. FactoMineR: an R package for multivariate analysis. J. Stat. Softw. 25, 1–18. https://doi.org/10.18637/JSS.V025.I01

Lei, P., Zhong, H., Duan, D., Pan, K., 2019. A review on mercury biogeochemistry in mangrove sediments: Hotspots of methylmercury production? Sci. Total Environ. 680, 140–150. https://doi.org/10.1016/j.scitotenv.2019.04.451

Leschine, S., Paster, B., Canale-Parola, E., 2006. Free-living saccharolytic spirochetes: the genus Spirochaeta.The prokaryotes, 3rd ed, vol 7 Springer, New York, pp. 195–210.

https://doi.org/10.1007/0-387-30747-8_7

Li, R., Tong, T., Wu, S., Chai, M., Xie, S., 2019. Multiple factors govern the biogeographic distribution of archaeal community in mangroves across China. Estuar. Coast. Shelf Sci. 231, 106414. https://doi.org/10.1016/j.ecss.2019.106414

Liang, J. Bin, Chen, Y.Q., Lan, C.Y., Tam, N.F.Y., Zan, Q.J., Huang, L.N., 2007. Recovery of novel bacterial diversity from mangrove sediment. Mar. Biol. 150, 739–747. https://doi.org/10.1007/s00227-006-0377-2

Liu, Y., Wei, X., Guo, X., Niu, D., Zhang, J., Gong, X., Jiang, Y., 2012. The long-term effects of reforestation on soil microbial biomass carbon in sub-tropic severe red soil degradation areas. Forest Ecol. and Manage. 285, 77–84.

Lloyd, K.G., Schreiber, L., Petersen, D.G., Kjeldsen, K.U., Lever, M.A., Steen, A.D., Stepanauskas, R., Richter, M., Kleindienst, S., Lenk, S., Schramm, A., Jorgensen, B.B., 2013. Predominant archaea in marine sediments degrade detrital proteins. Nature 496, 215–218. https://doi.org/10.1038/nature12033

Long, E.R., Macdonald, D.D., Smith, S.L., Calder, F.D., 1995. Incidence of adverse biological effects within ranges of chemical concentrations in marine and estuarine sediments. Environ. Manage. 19, 81–97. https://doi.org/10.1007/BF02472006

Luis, P., Saint-Genis, G., Vallon, L., Bourgeois, C., Bruto, M., Marchand, C., Record, E., Hugoni, M., 2019. Contrasted ecological niches shape fungal and prokaryotic community structure in mangroves sediments. Environ. Microbiol. 21, 1407–1424. https://doi.org/10.1111/1462-2920.14571

MacDonald, D.D., Dipinto, L.M., Field, J., Ingersoll, C.G., Long, E.R., Swartz, R.C., 2000. Development and evaluation of consensus-based sediment effect concentrations for polychlorinated biphenyls. Environ. Toxicol. Chem. 19, 1403–1413. https://doi.org/10.1002/etc.5620190524

960 Mangiafico, S., 2021. rcompanion: Functions to Support Extension Education
961 Program Evaluation. R package version 2.4.0.
962 https://CRAN.Rproject.org/package=rcompanion
963 Marchand, C., Lallier-Vergès, E., Baltzer, F., 2003. The composition of sedimentary organic
964 matter in relation to the dynamic features of a mangrove-fringed coast in French
965 Guiana. Estuar. Coast. Shelf Sci. 56, 119–130.
966 https://doi.org/10.1016/S0272-7714(02)00134-8
967 Marchand, C., Baltzer, F., Lallier-Vergès, E., Albéric, P., 2004. Pore-water chemistry in
968 mangrove sediments: Relationship with species composition and developmental stages
969 (French Guiana). Mar. Geol. 208, 361–381.
970 https://doi.org/10.1016/j.margeo.2004.04.015
971 Marchand, C., Lallier-Vergès, E., Baltzer, F., Albéric, P., Cossa, D., Baillif, P., 2006. Heavy
972 metals distribution in mangrove sediments along the mobile coastline of French Guiana.
973 Mar. Chem. 98, 1–17. https://doi.org/10.1016/j.marchem.2005.06.001
974 Marshall, I.P.G., Starnawski, P., Cupit, C., Fernández Cáceres, E., Ettema, T.J.G., Schramm,
975 A., Kjeldsen, K.U., 2017. The novel bacterial phylum Calditrichaeota is diverse,
976 widespread and abundant in marine sediments and has the capacity to degrade detrital
977 proteins: Expansion of Calditrichaeota diversity. Environ. Microbiol. Rep. 9, 397–403.
978 https://doi.org/10.1111/1758-2229.12544
979 Massel, S.R., Furukawa, K., Brinkman, R.M., 1999. Surface wave propagation in mangrove
980 forests, Fluid Dynamics Research. https://doi.org/10.1016/S0169-5983(98)00024-0
981 Matturro, B., Ubaldi, C., Rossetti, S., 2016. Microbiome dynamics of a polychlorobiphenyl
982 (PCB) historically contaminated marine sediment under conditions promoting reductive
983 dechlorination. Front. in Microbiol. 7, 1502. https://doi.org/10.3389/fmicb.2016.01502
984 Matturro, B., Mascolo, G., Rossetti, S., 2020. Microbiome changes and oxidative capability of

985 an anaerobic PCB dechlorinating enrichment culture after oxygen exposure. Nat.
986 Biotechnol. 56, 96–102. https://doi.org/10.1016/j.nbt.2019.12.004
987 McBride M.J., 2014. The Family *Flavobacteriaceae*. In: Rosenberg E., DeLong E.F., Lory S.,
988 Stackebrandt E., Thompson F. (eds) The Prokaryotes. Springer, Berlin, Heidelberg.
989 https://doi.org/10.1007/978-3-642-38954-2_130
990 McMurdie, P.J., Holmes, S., 2013. Phyloseq: an R package for reproducible interactive
991 analysis and graphics of microbiome census data. PLoS One 8, e61217.
992 https://doi.org/10.1371/journal.pone.0061217
993 Mendes, L.W., Taketani, R.G., Navarrete, A.A., Tsai, S.M., 2012. Shifts in phylogenetic
994 diversity of archaeal communities in mangrove sediments at different sites and depths in
995 southeastern Brazil. Res. Microbiol. 163, 366–377.
996 https://doi.org/10.1016/j.resmic.2012.05.005
997 Meng, J., Xu, J., Qin, D., He, Y., Xiao, X., Wang, F., 2014. Genetic and functional properties
998 of uncultivated MCG archaea assessed by metagenome and gene expression analyses.
999 ISME J. 8, 650–659. https://doi.org/10.1038/ismej.2013.174
1000 Michelet, C., Zeppilli, D., Hubas, C., Baldrighi, E., Cuny, P., Dirberg, G., Militon, C.,
1001 Walcker, R., Lamy, D., Jézéquel, R., Receveur, J., Gilbert, F., Houssainy, A. El, Dufour,
1002 A., Heimbürger-Boavida, L. E., Bihannic, I., Sylvi, L., Vivier, B., Michaud, E., 2021.
1003 First assessment of the benthic meiofauna sensitivity to low human-impacted mangroves
1004 in French Guiana. Forests 12, 338. https://doi.org/10.3390/f12030338
1005 Mohapatra, B., Phale, P. S., 2021. Microbial Degradation of Naphthalene and Substituted
1006 Naphthalenes: Metabolic Diversity and Genomic Insight for Bioremediation. Front.
1007 bioeng. 9, 1–28. https://doi.org/10.3389/fbioe.2021.602445
1008 Nakagawa, T., Stahl, D.A., 2013. Transcriptional response of the archaeal ammonia oxidizer
1009 Nitrosopumilus maritimus to low and environmentally relevant ammonia concentrations.

1010 Appl. Environ. Microbiol. 79, 6911–6916. https://doi.org/10.1128/AEM.02028-13
1011 Nicol, G. W., Leininger, S., Schleper, C., Prosser, J. I., 2008. The influence of soil pH on the
1012 diversity, abundance and transcriptional activity of ammonia oxidizing archaea and
1013 bacteria. Environ. Microbiol., 10. 2966–2978.
1014 https://doi.org/10.1111/j.1462-2920.2008.01701.x
1015 Nogueira, V.L.R., Rocha, L.L., Colares, G.B., Angelim, A.L., Normando, L.R.O., Cantão,
1016 M.E., Agnez-Lima, L.F., Andreote, F.D., Melo, V.M.M., 2015. Microbiomes and
1017 potential metabolic pathways of pristine and anthropized Brazilian mangroves. Reg.
1018 Stud. Mar. Sci. 2, 56–64. https://doi.org/10.1016/j.rsma.2015.08.008
1019 Oksanen, J., Blanchet, F.G., Friendly M., Kindt, R., Legendre, P., McGlinn, D., Minchin, P.
1020 R., O'Hara, R. B., Simpson, G.L., Solymos, P., Stevens, M. H. H., Szoecs, E, Wagner,
1021 H., 2020. Vegan: community ecology package. R package version 2.5-7.
1022 https://CRAN.R-project.org/package=vegan
1023 OSPAR, 2009. Background document on CEMP assessment criteria for QSR 2010. OSPAR
1024 Commission. London. Publication 461/2009. 25 pp.
1025 Parada, A.E., Needham, D.M., Fuhrman, J.A., 2016. Every base matters: assessing small
1026 subunit rRNA primers for marine microbiomes with mock communities, time series and
1027 global field samples: primers for marine microbiome studies. Environ. Microbiol. 18,
1028 1403–1414. https://doi.org/10.1111/1462-2920.13023
1029 Peixoto, R., Chaer, G.M., Carmo, F.L., Araújo, F. V., Paes, J.E., Volpon, A., Santiago, G.A.,
1030 Rosado, A.S., 2011. Bacterial communities reflect the spatial variation in pollutant levels
1031 in Brazilian mangrove sediment. Antonie van Leeuwenhoek, Int. J. Gen. Mol. Microbiol.
1032 99, 341–354. https://doi.org/10.1007/s10482-010-9499-0
1033 Pereira, G.M., Ellen da Silva Caumo, S., Mota do Nascimento, E.Q., Parra, Y.J., de Castro
1034 Vasconcellos, P., 2019. Polycyclic aromatic hydrocarbons in tree barks, gaseous and

1035 particulate phase samples collected near an industrial complex in São Paulo (Brazil).
1036 Chemosphere 237, 124499. https://doi.org/10.1016/j.chemosphere.2019.124499
1037 Pester, M., Schleper, C., Wagner, M., 2011. The Thaumarchaeota: An emerging view of their
1038 phylogeny and ecophysiology. Curr. Opin. Microbiol. 14, 300–306.
1039 https://doi.org/10.1016/j.mib.2011.04.007
1040 Pester, M., Rattei, T., Flechl, S., Gröngröft, A., Richter, A., Overmann, J., Reinhold-Hurek,
1041 B., Loy, A., Wagner, M., 2012. amoA-based consensus phylogeny of ammonia-oxidizing
1042 archaea and deep sequencing of amoA genes from soils of four different geographic
1043 regions: Archaeal amoA phylogeny and diversity in soils. Environ. Microbiol. 14,
1044 525–539. https://doi.org/10.1111/j.1462-2920.2011.02666.x
1045 Pichler, N., Maria de Souza, F., Ferreira dos Santos, V., Martins, C.C., 2021. Polycyclic
1046 aromatic hydrocarbons (PAHs) in sediments of the amazon coast: Evidence for localized
1047 sources in contrast to massive regional biomass burning. Environ. Pollut. 268, 115958.
1048 https://doi.org/10.1016/j.envpol.2020.115958
1049 Pinto, O.H.B., Silva, T.F., Vizzotto, C.S., Santana, R.H., Lopes, F.A.C., Silva, B.S.,
1050 Thompson, F.L., Kruger, R.H., 2020. Genome-resolved metagenomics analysis provides
1051 insights into the ecological role of Thaumarchaeota in the Amazon River and its plume.
1052 BMC Microbiol. 20, 1–11. https://doi.org/10.1186/s12866-020-1698-x
1053 Poltera, C., 2007. Agriculture: Pesticides Disrupt Nitrogen Fixation. J. Environ. Health, 115.
1054 1825. https://doi.org/10.1289/ehp.115-a579a
1055 Praveckova, M., Brennerova, M. V., Holliger, C., De Alencastro, F., Rossi, P., 2016. Indirect
1056 evidence link PCB dehalogenation with geobacteraceae in anaerobic sediment-free
1057 microcosms. Front. Microbiol. 7, 933. https://doi.org/10.3389/fmicb.2016.00933
1058 Quast, C., Pruesse, E., Yilmaz, P., Gerken, J., Schweer, T., Yarza, P., Peplies, J., Glöckner,
1059 F.O., 2013. The SILVA ribosomal RNA gene database project: improved data processing

and web-based tools. Nucleic Acids Res. 41, 590–596. https://doi.org/10.1093/nar/gks1219

Quero, G.M., Cassin, D., Botter, M., Perini, L., Luna, G.M., 2015. Patterns of benthic bacterial diversity in coastal areas contaminated by heavy metals, polycyclic aromatic hydrocarbons (PAHs) and polychlorinated biphenyls (PCBs). Front. Microbiol. 6, 1053. https://doi.org/10.3389/fmicb.2015.01053

Ramanathan, A.L., Singh, G., Majumdar, J., Samal, A.C., Chauhan, R., Ranjan, R.K., Rajkumar, K., Santra, S.C., 2008. A study of microbial diversity and its interaction with nutrients in the sediments of Sundarban mangroves. Indian J. Mar. Sci. 37, 159–165.

Rigonato, J., Kent, A.D., Alvarenga, D.O., Andreote, F.D., Beirigo, R.M., Vidal-Torrado, P., Fiore, M.F., 2013. Drivers of cyanobacterial diversity and community composition in mangrove soils in south-east Brazil: Cyanobacteria inhabiting mangrove soil. Environ. Microbiol. 15, 1103–1114. https://doi.org/10.1111/j.1462-2920.2012.02830.x

Rocha, L.L., Colares, G.B., Nogueira, V.L.R., Paes, F.A., Melo, V.M.M., 2016. Distinct habitats select particular bacterial communities in mangrove sediments. Int. J. Microbiol. 3435809. https://doi.org/10.1155/2016/3435809

Sackett, J. D., Kruger, B. R., Becraft, E. D., Jarett, J. K., Stepanauskas, R., Woyke, T., Moser, D. P., 2019. Four Draft Single-Cell Genome Sequences of Novel, Nearly Identical Kiritimatiellaeota Strains Isolated from the Continental Deep Subsurface. Microbiol. Resour. Announc, 8. https://doi.org/10.1128/mra.01249-18

Sangwan, N., Lata, P., Dwivedi, V., Singh, A., Niharika, N., Kaur, J., Anand, S., Malhotra, J., Jindal, S., Nigam, A., Lal, D., Dua, A., Saxena, A., Garg, N., Verma, M., Kaur, J., Mukherjee, U., Gilbert, J. A., Dowd, S. E., …, Lal, R., 2012. Comparative Metagenomic Analysis of Soil Microbial Communities across Three Hexachlorocyclohexane Contamination Levels. PLoS ONE 7, 1–12.

https://doi.org/10.1371/journal.pone.0046219

Santana, C.O., Spealman, P., Melo, V.M.M., Gresham, D., Jesus, T.B., Chinalia, F.A., 2019. Microbial community structure and ecology in sediments of a pristine mangrove forest. bioRxiv 2019814–833 . https://doi.org/10.1101/833814

Sarkar, D. ,2008. Lattice: Multivariate Data Visualization with R.

Sessitsch, A., Weilharter, A., Gerzabek, M. H., Kirchmann, H., & Kandeler, E., 2001. Microbial Population Structures in Soil Particle Size Fractions of a Long-Term Fertilizer Field. Appl. Environ. Microbiol., 67. 4215–4224. https://doi.org/10.1128/AEM.67.9.4215-4224.2001

Spalding, M., 2010. World atlas of mangroves. Routledge. Springer, New York.

Sheng, Y., Wang, G., Hao, C., Xie, Q., Zhang, Q., 2016. Microbial community structures in petroleum contaminated soils at an oil field, Hebei, China. Clean - Soil, Air, Water, 44, 829–839. https://doi.org/10.1002/clen.201500142

Strauss, E.A., Lamberti, G.A., 2000. Regulation of nitrification in aquatic sediments by organic carbon. Limnol. Oceanogr. 45, 1854–1859. https://doi.org/10.4319/lo.2000.45.8.1854

Takayasu, L., Suda, W., Hattori, M., 2019. Mapping the environmental microbiome. Encyclopedia of Bioinformatics and Computational Biology: ABC of Bioinformatics, 1–3, 17–28. https://doi.org/10.1016/B978-0-12-809633-8.20071-X

Tanner, M.A., Everett, C.L., Coleman, W.J., Yang, M.M., Youvan, D.C., 2000. Complex microbial communities inhabiting sulfide-rich black mud from marine coastal environments. Biotechnol. alia 8, 1–16.

Tavares, T. C. L., Bezerra, W. M., Normando, L. R. O., Rosado, A. S., Melo, V. M. M., 2021. Brazilian Semi-Arid Mangroves-Associated Microbiome as Pools of Richness and Complexity in a Changing World. Front. Microbiol., 12, 1–18.

https://doi.org/10.3389/fmicb.2021.715991

Tejada, M., García, C., Hernández, T., Gómez, I., 2015. Response of Soil Microbial Activity and Biodiversity in Soils Polluted with Different Concentrations of Cypermethrin Insecticide. AECT 69. https://doi.org/10.1007/s00244-014-0124-5

Terrat, S., Christen, R., Dequiedt, S., Lelièvre, M., Nowak, V., Regnier, T., Bachar, D., Plassart, P., Wincker, P., Jolivet, C., Bispo, A., Lemanceau, P., Maron, P.-A., Mougel, C., Ranjard, L., 2012. Molecular biomass and MetaTaxogenomic assessment of soil microbial communities as influenced by soil DNA extraction procedure: Soil DNA extraction impact on bacterial diversity. Microb. Biotechnol. 5, 135–141. https://doi.org/10.1111/j.1751-7915.2011.00307.x

Torres, G. G., Figueroa-Galvis, I., Muñoz-García, A., Polanía, J., & Vanegas, J., 2019. Potential bacterial bioindicators of urban pollution in mangroves. Environ. Pollut. 255, 113293. https://doi.org/10.1016/j.envpol.2019.113

Van Vliet, D.M., Ayudthaya, S.P.N., Diop, S., Villanueva, L., Stams, A.J.M., Sánchez-Andrea, I., 2019. Anaerobic degradation of sulfated polysaccharides by two novel Kiritimatiellales strains isolated from black sea sediment. Front. Microbiol. 10, 1–16. https://doi.org/10.3389/fmicb.2019.00253

Walcker, R., Gandois, L., Proisy, C., Corenblit, D., Mougin, É., Laplanche, C., Ray, R., Fromard, F., 2018. Control of “blue carbon” storage by mangrove ageing: Evidence from a 66-year chronosequence in French Guiana. Glob. Chang. Biol. 24, 2325–2338. https://doi.org/10.1111/gcb.14100

Wang, H., Wang, B., Dong, W., Hu, X., 2016. Co-acclimation of bacterial communities under stresses of hydrocarbons with different structures. Sci. Rep. 6. https://doi.org/10.1038/srep34588

Wang, B., Qin, W., Ren, Y., Zhou, X., Jung, M.Y., Han, P., Eloe-Fadrosh, E.A., Li, M.,

Zheng, Y., Lu, L., Yan, X., Ji, J., Liu, Y., Liu, L., Heiner, C., Hall, R., Martens-Habbena, W., Herbold, C.W., Rhee, S. keun, Bartlett, D.H., Huang, L., Ingalls, A.E., Wagner, M., Stahl, D.A., Jia, Z., 2019. Expansion of Thaumarchaeota habitat range is correlated with horizontal transfer of ATPase operons. ISME J. 13, 3067–3079. https://doi.org/10.1038/s41396-019-0493-x

Wardle, D. A., 1992. A comparative assessment of factors which influence microbial biomass carbon and nitrogen levels in soil. Biol. rev. biol. proc. Camb. Philos. Soc. 67, 321–358. https://doi.org/10.1111/j.1469-185X.1992.tb00728.x

Wu, Y., Zhang, J., Liu, S.M., Zhang, Z.F., Yao, Q.Z., Hong, G.H., Cooper, L., 2007. Sources and distribution of carbon within the Yangtze River system. Estuar. Coast. Shelf Sci. 71, 13–25. https://doi.org/10.1016/j.ecss.2006.08.016

Wu, X. H., Zhang, Y., Du, P. Q., Xu, J., Dong, F. S., Liu, X. G., Zheng, Y. Q., 2018. Impact of fomesafen on the soil microbial communities in soybean fields in Northeastern China. Ecotoxicol Environ Saf 148, 169–176. https://doi.org/10.1016/j.ecoenv.2017.10.00

Xiang, X., Wang, R., Wang, H., Gong, L., Man, B., Xu, Y., 2017. Distribution of Bathyarchaeota communities across different terrestrial settings and their potential ecological functions. Sci. Rep. 7, 1–11. https://doi.org/10.1038/srep45028

Yin, X., Cai, M., Liu, Y., Zhou, G., Richter-Heitmann, T., Aromokeye, D.A., Kulkarni, A.C., Nimzyk, R., Cullhed, H., Zhou, Z., Pan, J., Yang, Y., Gu, J.D., Elvert, M., Li, M., Friedrich, M.W., 2021. Subgroup level differences of physiological activities in marine Lokiarchaeota. ISME J. 15, 848–861. https://doi.org/10.1038/s41396-020-00818-5

Youssef, N., H., Farag, I.F., Rinke, C., Hallam, S.J., Woyke, T., Elshahed, M.S., 2015. In silico analysis of the metabolic potential and niche specialization of candidate phylum "Latescibacteria" (WS3). PLoS One 10, e0127499. https://doi.org/10.1371/journal.pone.0127499

Yu, T., Liang, Q., Niu, M., Wang, F., 2017. High occurrence of Bathyarchaeota (MCG) in the deep-sea sediments of South China Sea quantified using newly designed PCR primers: Diversity and abundance of Bathyarchaeota. Environ. Microbiol. Rep. 9, 374–382. https://doi.org/10.1111/1758-2229.12539

Zeng, Y., Nupur, Y., Wu, N., Madsen, A. M., Chen, X., Gardiner, A. T., Koblížek, M., 2021. Gemmatimonas groenlandica sp. nov. Is an Aerobic Anoxygenic Phototroph in the Phylum Gemmatimonadetes. Front. Microbiol., 11, 1–18. https://doi.org/10.3389/fmicb.2020.606612

Zhang, X. Z., Xie, J. J., & Sun, F. L., 2014. Effects of three polycyclic aromatic hydrocarbons on sediment bacterial community. Curr. Microbiol. 68, 756–762. https://doi.org/10.1007/s00284-014-0535-6

Zhang, X., Hu, B.X., Ren, H., Zhang, J., 2018. Composition and functional diversity of microbial community across a mangrove-inhabited mudflat as revealed by 16S rDNA gene sequences. Sci. Total Environ. 633, 518–528. https://doi.org/10.1016/j.scitotenv.2018.03.158

Zhang, C.-J., Pan, J., Duan, C.-H., Wang, Y.-M., Liu, Y., Sun, J., Zhou, H.-C., Song, X., Li, M., 2019. Prokaryotic Diversity in Mangrove Sediments across Southeastern China Fundamentally Differs from That in Other Biomes. MSystems 4. https://doi.org/10.1128/msystems.00442-19

Zhou, Z., Meng, H., Liu, Y., Gu, J.D., Li, M., 2017. Stratified bacterial and archaeal community in mangrove and intertidal wetland mudflats revealed by high throughput 16S rRNA gene sequencing. Front. Microbiol. 8, 1–19. https://doi.org/10.3389/fmicb.2017.02148

Zhou, Z., Pan, J., Wang, F., Gu, J.D., Li, M., 2018. Bathyarchaeota: Globally distributed metabolic generalists in anoxic environments. FEMS Microbiol. Rev. 42, 639–655.

https://doi.org/10.1093/femsre/fuy023

Zhou, Z., Liu, Y., Lloyd, K.G., Pan, J., Yang, Y., Gu, J.D., Li, M., 2019. Genomic and transcriptomic insights into the ecology and metabolism of benthic archaeal cosmopolitan, Thermoprofundales (MBG-D archaea). ISME J. 13, 885–901. https://doi.org/10.1038/s41396-018-0321-8

Figures legends :

Figure 1. Location of mangrove sampling stations in FG (South America). S1 is located near Cayenne city, S2 at the confluence of Cayenne and Montsinery Rivers, and S3 along the Cayenne River. Mangrove cover is represented in green. (modified from Michelet et al., 2021).

Figure 2. Multiple factor analysis of data obtained from different stations with four groups of variables ($cos^2 > 0.5$): physicochemical parameters (green), OM (orange), organic contaminants (purple), and TMM (blue). Graphs represent (A,C) individual factor plots and (B,D) correlation plots on axes 1 and 2 (A,B) and 1 and 3 (C,D). Dots correspond to 26 samples from three sampling stations: S1 (green), S2 (blue), S3 (red). A, B, C indicate replicates; 1: 0-2 cm; 2: 2-10 cm; 3: > 10 cm.

Figure 3. Z-score heatmap of top 30 phyla (representing 94.3% of total community) at three sampling stations (S1, S2, S3). Red indicates higher Z-scores (higher relative abundance compared to mean of abundance of that phylum) and blue indicates lower Z-scores (lower relative abundance).

Figure 4. Spearman's rank correlation coefficient heatmap showing relationships between environmental variables and interesting taxa. A: phylum level; B: family level. Statistically significant Spearman correlations are highlighted (*$p < 0.05$, **$p < 0.01$, ***$p < 0.001$).

Table legend:

Table 1. Levels of organic contaminants and metals in sediments at three depths (0-2, 2-10, > 10 cm) at three sampling stations (mean ± SD, n = 3). Bold numbers correspond to values superior to OSPAR ERL or NOAA threshold.

Supplementary Data A: Concentrations of TMM in the blank (µg L-1) and calculated limits of detection (LOD) and quantification (LOQ) (µg L-1) for water samples.

Element	blank	LOD	LOQ
Ag	0.002	0.001	0.003
Al	0.5	0.3	1
As	0.002	0.003	0.01
Ba	0.02	0.005	0.015
Be	0.001	0.001	0.003
Bi	0.002	0.001	0.003
Cd	0.001	0.001	0.003
Co	0.001	0.002	0.006
Cr	0.005	0.003	0.01
Cs	0.001	0.001	0.003
Cu	0.02	0.01	0.03
Fe	0.02	0.02	0.06
Li	0.005	0.002	0.006
Mn	0.005	0.003	0.01
Mo	0.005	0.003	0.01
Ni	0.001	0.001	0.003
Pb	0.001	0.001	0.003
Rb	0.005	0.003	0.01
Sb	0.001	0.002	0.006
Sn	0.002	0.001	0.003
Sr	0.02	0.01	0.03
Ti	0.05	0.03	0.1
U	0.001	0.001	0.003
V	0.002	0.002	0.006
Zn	0.010	0.005	0.015

Supplementary data B: Averaged physicochemical characteristics over depth (0-2 cm; 2-10 cm; > 10 cm) from the three sampling stations (mean ± SD, n=3).

	Station 1			Station 2			Station 3		
Depth	0-2 cm	2-10 cm	> 10 cm	0-2 cm	2-10 cm	> 10 cm	0-2 cm	2-10 cm	> 10 cm
	Physicochemical parameters								
pH	6.0 ± 0.1	6.3 ± 0.0	6.5 ± 0.1	6.4 ± 0.2	6.2 ± 0.2	6.5 ± 0.1	6.4 ± 0.1	6.0 ± 0.3	5.7 ± 0.1
Redox potential (mV)	198 ± 34.6	177.6 ± 16.8	26.1 ± 39.3	-142.5 ± 55.5	-50.3 ± 61.5	-77.6 ± 24.8	165.0 ± 15.2	152.6 ± 11.9	164.7 ± 14.7
	Granulometry (%)								
Clay	1.9 ± 0.7	3.9 ± 1.0	4.9 ± 0.8	8.0 ± 1.1	8.1 ± 0.4	8.6 ± 0.8	7.8 ± 1.3	6.7 ± 0.5	7.2 ± 0.2
Silt	76.1 ± 4.5	73.7 ± 3.0	76.1 ± 0.9	88.7 ± 2.6	86.4 ± 1.3	85.8 ± 2.0	88.9 ± 1.3	87.8 ± 2.1	88.2 ± 1.7
Sand	20.9 ± 4.6	21.5 ± 4.0	18.2 ± 0.8	3.0 ± 1.5	5.1 ± 1.1	5.3 ± 2.1	3.0 ± 0.3	5.0 ± 2.5	2.2 ± 1.7
	Carbon TC and nitrogen TN contents								
TC (%)	5.5 ± 1.3	3.0 ± 0.4	2.5 ± 0.3	1.7 ± 0.3	1.9 ± 0.4	1.3 ± 0.4	1.5 ± 0.2	1.3 ± 0.2	1.7 ± 0.2
TN (%)	0.3 ± 0.1	0.2 ± 0.0	0.2 ±0.01	0.2 ± 0.15	0.2 ±0.03	0.1± 0.01	0.2 ± 0.01	0.2 ± 0.01	0.1 ± 0.01
TC:TN (mol/mol)	17.9 ± 2.1	14.3 ± 1.3	15.1 ± 1.5	9.8 ± 0.8	11.5± 1.2	9.7 ± 0.7	9.7 ± 0.4	9.7 ± 0.2	9.1 ± 0.5

Supplementary data C: Values of the molecular microbial biomass, bacterial and archaeal 16S rRNA gene copies number and alpha diversity indexes (specific richness and Shannon index) at each station and for the different depth layers (mean ± SD; n=3).

	Station 1			**Station 2**			**Station 3**		
Depth	**0-2 cm**	**2-10 cm**	**> 10cm**	**0-2 cm**	**2-10 cm**	**> 10cm**	**0-2 cm**	**2-10 cm**	**> 10cm**
Molecular microbial biomass (µg g^{-1} d.w.)	3.67 ± 0.35	2.38 ± 1.31	2.07 ± 0.11	7.34 ± 0.86	2.73 ± 1.45	2.40 ± 0.36	3.98 ± 0.52	3.26 ± 0.23	2.40 ± 0.04
	Prokaryotic abundance estimation (16S rRNA copies g^{-1} d.w.)								
Bacterial 16S rRNA genes	$7.9 \times 10^9 \pm 4.4 \times 10^9$	$2.3 \times 10^9 \pm 1.4 \times 10^9$	$1.5 \times 10^9 \pm 6.2 \times 10^8$	$1.4 \times 10^9 \pm 1.3 \times 10^8$	$2.4 \times 10^8 \pm 1.7 \times 10^8$	$9.4 \times 10^7 \pm 4.8 \times 10^7$	$4.9 \times 10^8 \pm 1.8 \times 10^8$	$4.0 \times 10^8 \pm 5.6 \times 10^7$	$2.6 \times 10^8 \pm 1.4 \times 10^8$
Archaeal 16S rRNA genes	$5.8 \times 10^6 \pm 3.1 \times 10^6$	$4.1 \times 10^6 \pm 1.6 \times 10^6$	$6.6 \times 10^6 \pm 3.7 \times 10^6$	$2.5 \times 10^7 \pm 1.7 \times 10^7$	$8.0 \times 10^6 \pm 6.1 \times 10^6$	$2.5 \times 10^6 \pm 9.6 \times 10^5$	$5.2 \times 10^6 \pm 3.1 \times 10^6$	$3.1 \times 10^6 \pm 1.2 \times 10^6$	$4.9 \times 10^6 \pm 6.0 \times 10^6$
	Alpha diversity index								
Specific richness	352 ± 128	539 ± 40	643 ± 213	437 ± 193	515 ± 227	458 ± 220	354 ± 122	431 ± 120	480 ± 144
Shannon index	5.5 ± 0.3	6.0 ± 0.1	6.1 ± 0.4	5.7 ± 0.5	5.8 ± 0.5	5.7 ± 0.4	5.5 ± 0.3	5.8 ± 0.3	5.9 ± 0.3

Supplementary data D: Histogram of the relative abundance of the top 30 phyla at each station and for the different depth layers (mean ± SD; n =3). The p-values represent the significant differences of taxa relative abundances between station (*p = 0.05, **p= 0.01, ***p=0.001).

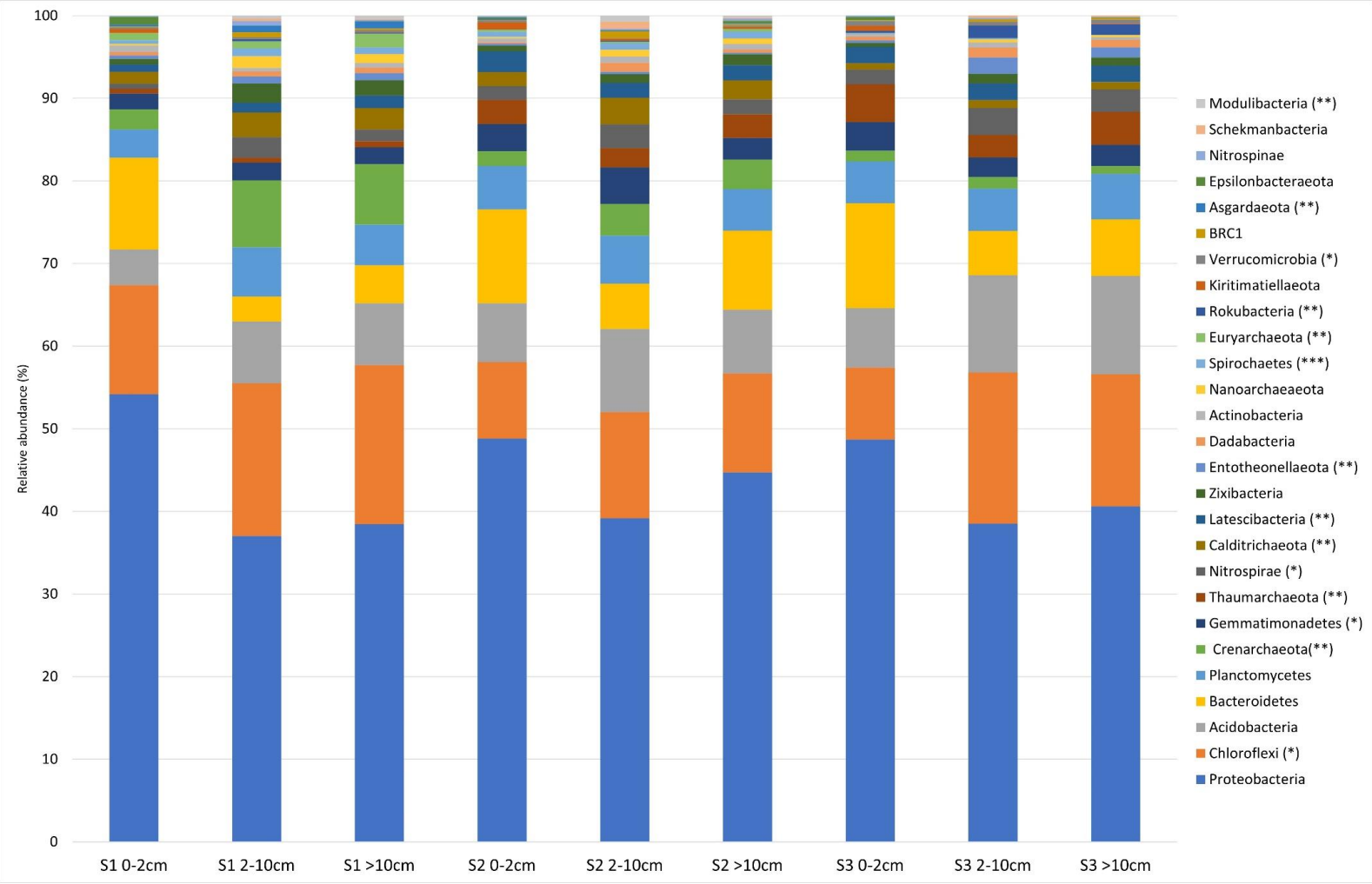

Supplementary data E: Relative abundances of the top 50 families at each station over depth (L1: 0-2 cm; L2; 2-10 cm; L3: > 10 cm) (mean ± SD; n = 3).

Family	S1L1	S1L2	S1L3	S2L1	S2L2	S2L3	S3L1	S3L2	S3L3
Desulfobacteraceae	3.43 ± 0.18	5 ± 0.37	6.4 ± 1.02	3.97 ±1.72	4.71 ±1.83	5.24 ± 1.4	1.32 ±0.37	1.08 ±0.52	1.89 ± 0.78
Syntrophobacteraceae	0.44 ± 0.17	1.18 ± 0.06	1.26 ± 0.09	0.19 ± 0.05	0.33 ± 0.16	0.8 ± 0.47	0.15 ± 0.03	0.22 ± 0.05	0.15 ± 0.14
Anaerolineaceae	1.99 ± 0.54	2.64 ± 0.76	2.11 ± 0.12	0.97 ± 0.32	1.72 ± 0.91	1.79 ± 0.47	1.71 ± 0.56	3.48 ± 1.26	3.74 ± 1.01
Desulfobulbaceae	3.28 ± 0.1	1.84 ± 0.01	2.61 ± 1.11	3.88 ± 0.78	4.38 ± 0.74	2.26 ± 1.33	2.26 ± 0.63	2.14 ± 0.47	2.29 ± 0.81
Nitrosopumilaceae	0.23 ± 0.14	0.16 ± 0.09	0.07 ± 0.02	2.4 ± 0.39	1.37 ± 1.54	1.05 ± 1.25	2.24 ± 0.09	2.58 ± 0.49	1.5 ± 0.43
Xanthobacteraceae	1.09 ± 0.34	1.38 ± 0.59	0.96 ± 0.45	0 ± 0	0.06 ± 0.06	0.13 ± 0.12	0.32 ± 0.46	0.9 ± 0.25	1.08 ± 0.09
Rhizobiales_IS	0.4 ± 0.1	0.78 ± 0.04	0.28 ± 0.23	0.03 ± 0.02	0.14 ± 0.08	0.04 ± 0.03	0.28 ± 0.08	0.47 ± 0.21	0.56 ± 0.17
TRA3-20	0.05 ± 0.09	0.09 ± 0.01	0.01 ± 0.02	0.13 ± 0.02	0.08 ± 0.06	0.09 ± 0.05	0.19 ± 0.06	0.51 ± 0.16	0.33 ± 0.13
Beggiatoaceae	0.53 ± 0.08	0.55 ± 0.22	0.3 ± 0.17	0 ± 0	0 ± 0	0 ± 0	0.08 ± 0.14	0.15 ± 0.14	0.09 ± 0.05
bacteriap25	0 ± 0	0.09 ± 0.13	0.13 ± 0.07	0 ± 0	0 ± 0	0.14 ± 0.15	0.06 ± 0.09	0.48 ± 0.26	0.89 ± 0.29
Kiloniellaceae	0.4 ± 0.27	0.72 ± 0.26	0.51 ± 0.46	0.84 ± 0.24	0.56 ± 0.22	0.76 ± 0.16	0.93 ± 0.24	1 ± 0.11	0.88 ± 0.04
Sva1033	0.27 ± 0.12	0 ± 0	0 ± 0	0.68 ± 0.1	0.74 ± 0.58	0.17 ± 0.3	0.53 ± 0.11	0.2 ± 0.2	0 ± 0
Mariprofundaceae	1.55 ± 0.73	0.37 ± 0.01	0.4 ± 0.27	0.11 ± 0.09	0.32 ± 0.3	0.28 ± 0.32	0 ± 0	0 ± 0	0.17 ± 0.27
Desulfarculaceae	0.64 ± 0.06	1.36 ± 0.05	2.21 ± 0.54	0.57 ± 0.07	0.74 ± 0.31	1.14 ± 0.36	0.49 ± 0.09	0.43 ± 0.13	0.58 ± 0.05
Calditrichaceae	0.55 ± 0.19	1.44 ± 0.18	1.97 ± 0.24	0.68 ± 0.14	1.3 ± 0.35	2.13 ± 0.9	0.44 ± 0.19	0.58 ± 0.23	0.69 ± 0.12
Spirochaetaceae	0.26 ± 0.03	0.36 ± 0.06	0.65 ± 0.43	0.43 ± 0.06	0.47 ± 0.08	0.55 ± 0.23	0.09 ± 0.07	0.04 ± 0.05	0.07 ± 0.07
Thioalkalispiraceae	1.13 ± 0.65	0.57 ± 0.15	1.08 ± 0.71	0.25 ± 0.04	0.63 ± 0.35	0.23 ± 0.21	0.21 ± 0.21	0.07 ± 0.09	0.1 ± 0.12
Vibrionaceae	0.32 ± 0.27	0.07 ± 0.1	0 ± 0	0.12 ± 0	0.04 ± 0.06	0.07 ± 0.12	0.49 ± 0.41	0.11 ± 0.12	0.02 ± 0.03
Gemmatimonadaceae	0.09 ± 0.15	0.58 ± 0	0.48 ± 0.25	0.2 ± 0.18	0.42 ± 0.16	0.98 ± 0.32	0.26 ± 0.26	0.63 ± 0.15	0.74 ± 0.17
Pirellulaceae	0.62 ± 0.41	0.99 ± 0.08	1.13 ± 0.81	0.29 ± 0.27	0.66 ± 0.06	0.78 ± 0.27	0.35 ± 0.38	0.74 ± 0.16	0.79 ± 0.27
Entotheonellaceae	0.18 ± 0.1	0.6 ± 0.14	0.61 ± 0.62	0.04 ± 0.06	0.12 ± 0.03	0.23 ± 0.14	0.09 ± 0.08	0.79 ± 0.15	1.28 ± 0.38
Nitrosomonadaceae	0.65 ± 0.25	0.53 ± 0.2	0.14 ± 0.08	0.16 ± 0.02	0.25 ± 0.01	0.16 ± 0.03	0.67 ± 0.46	1.11 ± 0.31	0.99 ± 0.29
Ectothiorhodospiraceae	0.27 ± 0.12	0.31 ± 0.3	0.19 ± 0.17	0 ± 0	0.08 ± 0.07	0.05 ± 0.09	0.05 ± 0.08	0 ± 0	0.06 ± 0.06
Desulfuromonadaceae	0.2 ± 0.2	0.09 ± 0.12	0.03 ± 0.06	0.21 ± 0.07	0.23 ± 0.07	0.21 ± 0.08	0.26 ± 0.19	0.3 ± 0.1	0.33 ± 0.14

KF-JG30-B3	0.12 ± 0.04	0.3 ± 0.04	0.07 ± 0.07	0.13 ± 0.11	0.1 ± 0.01	0.07 ± 0.08	0.24 ± 0.06	0.51 ± 0.28	0.25 ± 0.13
SG8-4	0.13 ± 0.12	0.18 ± 0.04	0.52 ± 0.18	0.09 ± 0.16	0.24 ± 0.4	0.38 ± 0.4	0.09 ± 0.08	0.06 ± 0.11	0.12 ± 0.11
Acidiferrobacteraceae	0.59 ± 0.11	0.52 ± 0.16	0.38 ± 0.12	0 ± 0	0.04 ± 0.05	0.03 ± 0.03	0.04 ± 0.07	0.34 ± 0.1	0.47 ± 0.22
Kiritimatiellaceae	0.2 ± 0.15	0.04 ± 0.05	0.03 ± 0.04	0.4 ± 0.08	0.09 ± 0.08	0.19 ± 0.15	0.28 ± 0.07	0.1 ± 0.1	0.03 ± 0.03
Moduliflexaceae	0.01 ± 0.02	0.05 ± 0.04	0.43 ± 0.39	0.07 ± 0.07	0.14 ± 0.13	0.56 ± 0.28	0 ± 0	0 ± 0	0 ± 0
Thermoanaerobaculaceae	0.58 ± 0.47	1.81 ± 0.11	1.23 ± 1.19	0.93 ± 0.15	1.19 ± 0.5	1.9 ± 0.86	0.47 ± 0.23	0.9 ± 0.26	1.21 ± 0.47
Nitrosococcaceae	0.03 ± 0.05	0.13 ± 0.06	0.05 ± 0.05	0.46 ± 0.04	0.27 ± 0.19	0.29 ± 0.07	0.28 ± 0.06	0.12 ± 0.05	0.14 ± 0.06
Thiohalorhabdaceae	0 ± 0	0 ± 0	0 ± 0	0.44 ± 0.16	0.11 ± 0.15	0.08 ± 0.13	0.24 ± 0.01	0.07 ± 0.08	0 ± 0
PHOS-HE36	0.23 ± 0.11	0.48 ± 0.07	0.4 ± 0.11	0.14 ± 0.25	0.59 ± 0.33	0.92 ± 0.38	0 ± 0	0.21 ± 0.06	0.39 ± 0.25
Prolixibacteraceae	0.4 ± 0.23	0.01 ± 0.01	0.01 ± 0.01	0.9 ± 0.15	0.66 ± 0.2	0.34 ± 0.27	0.35 ± 0.15	0.15 ± 0.06	0.23 ± 0.06
Rubinisphaeraceae	0.15 ± 0.09	0.09 ± 0.02	0.19 ± 0.2	0.03 ± 0.04	0 ± 0.01	0 ± 0	0.06 ± 0.1	0.19 ± 0.05	0.09 ± 0.08
Flavobacteriaceae	1.08 ± 0.43	0.05 ± 0.07	0.01 ± 0.01	1.67 ± 0.39	0.7 ± 0.61	0.38 ± 0.51	2.54 ± 1.38	0.33 ± 0.16	0.01 ± 0.01
SB-5	0.45 ± 0.44	0.46 ± 0.11	0.67 ± 0.48	0.21 ± 0.15	0.49 ± 0.1	0.35 ± 0.14	0 ± 0.01	0.06 ± 0.05	0.23 ± 0.07
Woeseiaceae	0.23 ± 0.16	0.22 ± 0.04	0.02 ± 0.02	2.17 ± 0.73	0.85 ± 0.58	0.75 ± 0.54	1.44 ± 0.22	0.48 ± 0.24	0.33 ± 0.13
Nitrospiraceae	0.01 ± 0.02	0 ± 0	0.14 ± 0.2	0.3 ± 0.09	0.15 ± 0.1	0.09 ± 0.12	0.35 ± 0.11	0.53 ± 0.14	0.59 ± 0.19
B1-7BS	0 ± 0	0 ± 0	0 ± 0	0.11 ± 0.03	0.07 ± 0.07	0.24 ± 0.09	0.16 ± 0.02	0.28 ± 0.09	0.3 ± 0.11
Solibacteraceae_Subgroup3	0.08 ± 0.02	0.15 ± 0.02	0.14 ± 0.09	0.03 ± 0.06	0.2 ± 0.1	0.18 ± 0.11	0.32 ± 0.2	0.41 ± 0.07	0.41 ± 0.13
Nitrincolaceae	0.33 ± 0.19	0.05 ± 0.03	0 ± 0	0.1 ± 0.12	0.08 ± 0.07	0 ± 0	0.65 ± 0.14	0.33 ± 0.13	0.1 ± 0.02
Gallionellaceae	0.44 ± 0.18	0.03 ± 0.02	0.12 ± 0.11	0 ± 0	0.05 ± 0.05	0.01 ± 0.01	0.1 ± 0.18	0.03 ± 0.06	0.1 ± 0.15
Phycisphaeraceae	0.08 ± 0.1	0.19 ± 0.09	0.21 ± 0.06	0.44 ± 0.24	0.2 ± 0.02	0.45 ± 0.18	0.49 ± 0.09	0.31 ± 0.03	0.36 ± 0.13
Ignavibacteriaceae	0.64 ± 0.34	0.31 ± 0.04	0.12 ± 0.09	0 ± 0.01	0.18 ± 0.08	0.08 ± 0.14	0 ± 0	0.2 ± 0.09	0.36 ± 0.2
Gimesiaceae	0.55 ± 0.18	0.57 ± 0.11	0.25 ± 0.18	0.15 ± 0.06	0.18 ± 0.12	0.15 ± 0.15	0.55 ± 0.38	0.57 ± 0.22	0.38 ± 0.17
A4b	0.34 ± 0.18	0.66 ± 0.09	0.39 ± 0.1	0.34 ± 0.17	0.2 ± 0.15	0.24 ± 0.07	0.66 ± 0.13	1.06 ± 0.44	0.94 ± 0.32
Sphingomonadaceae	0.4 ± 0.3	0.14 ± 0.04	0.07 ± 0.1	0.26 ± 0.05	0.2 ± 0.22	0.17 ± 0.16	0.63 ± 0.42	0.42 ± 0.19	0.17 ± 0.09
Stappiaceae	0 ± 0	0 ± 0	0 ± 0	0.25 ± 0.16	0.09 ± 0.1	0.12 ± 0.17	0.02 ± 0.04	0 ± 0	0.07 ± 0.12
Rhodobacteraceae	0.97 ± 0.3	0.02 ± 0.02	0 ± 0	0.67 ± 0.05	0.51 ± 0.37	0.24 ± 0.3	1.19 ± 0.4	0.38 ± 0.08	0.18 ± 0.08

Supplementary data F: Values of the Spearman's rank correlation coefficient between the environmental variables and the taxa at the phylum levels (*p = 0.05, **p= 0.01, ***p=0.001), HCB = Hexachlorobenzene, Naph = Naphthalene, Phen = Phenanthrene.

Phylum	Al	Cd111	CN	Cr	Ctot	ddd24	dde44	DBT	dieldrin	HCB	Hg	Mn	Mo95	Naph	Ntot	PCBs	Phen	Zn
Acidobacteria	0,2	-0,7 (**)	-0,7 (**)	0,3	-0,6 (**)	-0,1	-0,1	0,3	-0,3	-0,3	-0,2	0,4	-0,2	0,5	-0,6 (*)	-0,3	0,0	0,3
Actinobacteria	-0,4	0,5	0,4	-0,5	0,3	0,3	0,1	-0,2	0,4	0,2	0,1	-0,4	-0,1	-0,6 (*)	0,1	0,4	-0,1	-0,5
Altiarchaeota	-0,3	0,2	0,2	-0,3	0,1	-0,2	-0,1	-0,2	-0,1	0,2	0,3	-0,3	0,1	-0,2	0,0	0,0	-0,1	-0,3
AncK6	-0,4	0,3	0,3	-0,5	0,2	0,1	0,2	0,0	0,3	0,3	0,4	-0,5 (*)	0,2	-0,2	0,0	0,3	0,1	-0,4
Asgardaeota	-0,5	0,6 (*)	0,7 (***)	-0,6 (*)	0,7 (**)	0,0	0,2	-0,2	0,3	0,5	0,7 (**)	-0,8 (***)	0,6 (*)	-0,4	0,4	0,3	0,2	-0,5
Bacteroidetes	0,3	0,1	-0,1	0,2	0,0	0,0	-0,1	-0,2	-0,1	-0,2	-0,3	0,5	-0,2	-0,1	0,3	-0,1	-0,2	0,2
BRC1	-0,4	0,0	0,2	-0,2	0,2	0,1	0,1	0,2	0,0	0,1	0,3	-0,4	0,3	0,1	-0,1	0,1	0,2	-0,2
Calditrichaeota	-0,4	0,1	0,3	-0,4	0,1	0,5	0,5	0,0	0,7 (**)	0,7 (**)	0,0	-0,5	0,0	-0,4	-0,2	0,7 (**)	0,0	-0,5
Chlamydiae	-0,3	0,4	0,3	-0,4	0,3	0,1	0,2	0,0	0,3	0,0	0,2	-0,4	0,2	-0,2	0,2	0,2	0,0	-0,2
Chloroflexi	-0,3	0,2	0,3	-0,2	0,3	-0,2	0,0	0,1	-0,1	0,0	0,6 (*)	-0,6 (**)	0,5	0,1	0,0	-0,2	0,2	-0,1
CK-2C2-2	-0,2	0,3	0,2	-0,2	0,3	-0,2	-0,1	0,1	0,2	0,0	0,2	-0,3	0,2	-0,2	0,2	0,0	0,3	0,0
Crenarchaeota	-0,6 (*)	0,6 (*)	0,7 (***)	-0,5	0,6 (**)	0,2	0,2	-0,1	0,4	0,5	0,4	-0,9 (***)	0,3	-0,6 (*)	0,2	0,5	0,1	-0,5
Dadabacteria	0,0	-0,1	-0,2	0,2	-0,2	-0,2	-0,4	0,2	-0,3	-0,1	0,2	-0,2	0,1	0,2	-0,5	-0,3	0,2	0,1
Deinococcus-Thermus	-0,2	0,3	0,2	-0,3	0,2	0,2	0,0	0,1	0,1	0,1	0,0	-0,2	0,0	-0,1	0,2	0,2	0,3	-0,3
Dependentiae	-0,5	0,1	0,3	-0,4	0,2	0,1	0,0	-0,1	0,2	0,3	0,1	-0,3	0,0	-0,2	-0,1	0,2	0,1	-0,5
Diapherotrites	-0,2	0,3	0,3	-0,3	0,3	0,0	0,1	0,1	0,0	0,3	0,3	-0,3	0,3	-0,2	0,1	0,1	0,1	-0,2
Elusimicrobia	0,0	-0,2	-0,3	-0,2	-0,2	0,3	0,3	-0,2	0,3	0,3	-0,3	0,3	-0,3	-0,2	0,0	0,3	-0,3	0,0
Entotheonellaeota	0,0	-0,2	-0,2	0,1	-0,1	-0,3	-0,1	0,3	-0,4	-0,1	0,5	-0,2	0,4	0,4	-0,2	-0,4	0,3	0,1
Epsilonbacteraeota	0,0	0,1	0,1	-0,1	0,2	0,0	-0,1	-0,2	-0,1	-0,3	-0,2	0,3	-0,1	-0,1	0,4	-0,1	-0,1	0,0
Euryarchaeota	-0,5	0,7 (***)	0,8 (***)	-0,5	0,7 (**)	0,0	0,1	-0,3	0,3	0,4	0,6 (*)	-0,9 (***)	0,5	-0,5	0,4	0,2	0,1	-0,5
FCPU426	0,0	0,2	0,0	-0,1	0,0	0,0	-0,2	0,1	-0,2	0,0	0,1	0,0	-0,1	0,1	0,1	-0,1	0,2	0,0
Fibrobacteres	0,0	0,2	0,1	-0,1	0,1	0,0	0,0	0,0	0,3	0,3	-0,2	0,0	-0,1	-0,4	0,2	0,3	-0,2	-0,1
Firmicutes	-0,2	-0,1	0,1	-0,2	0,0	0,2	0,2	0,0	0,1	0,0	0,2	0,0	0,2	0,1	0,0	0,1	0,2	-0,2
Fusobacteria	-0,3	0,3	0,3	-0,3	0,2	0,4	0,4	0,0	0,3	0,2	0,2	-0,3	0,2	-0,1	0,3	0,4	0,1	-0,3
Gemmatimonadetes	0,2	-0,5	-0,3	0,2	-0,5	0,2	-0,1	0,0	0,2	0,2	-0,4	0,4	-0,5	0,1	-0,5	0,1	0,0	0,2
GN01	-0,3	0,1	0,2	-0,2	0,0	0,4	0,3	-0,1	0,5	0,5 (*)	0,1	-0,5	-0,1	-0,1	-0,3	0,4	0,0	-0,3

Hydrogenedentes	0,2	-0,4	-0,3	0,2	-0,3	-0,1	-0,1	0,0	-0,2	-0,3	0,0	0,3	-0,1	0,3	-0,1	-0,3	-0,1	0,2
Kiritimatiellaeota	0,4	0,1	-0,1	0,2	0,0	0,1	0,0	-0,2	0,1	0,1	-0,5	0,4	-0,3	-0,1	0,3	0,1	-0,2	0,2
Latescibacteria	0,6 (*)	-0,5	-0,6 (**)	0,5	-0,6 (*)	-0,2	-0,2	0,2	-0,1	-0,2	-0,5	0,6 (*)	-0,4	0,3	-0,3	-0,2	-0,1	0,5
LCP-89	-0,4	0,1	0,3	-0,4	0,1	0,3	0,3	0,0	0,4	0,5	0,2	-0,5 (*)	0,0	-0,1	-0,2	0,4	0,0	-0,4
Lentisphaerae	0,4	-0,3	-0,4	0,3	-0,4	0,2	0,1	0,2	0,1	-0,1	-0,6 (*)	0,6 (**)	-0,6 (*)	0,2	-0,1	0,1	0,0	0,4
Margulisbacteria	0,1	-0,2	-0,1	0,2	0,0	-0,2	-0,1	-0,2	-0,2	-0,2	0,1	0,1	0,2	0,2	0,0	-0,2	-0,3	0,2
Marinimicrobia	-0,2	0,3	0,3	-0,2	0,2	0,1	-0,1	-0,1	0,0	0,0	0,1	-0,4	0,1	-0,1	-0,1	0,1	0,0	-0,3
Modulibacteria	-0,3	0,3	0,3	-0,3	0,2	0,4	0,3	-0,2	0,7 (**)	0,7 (**)	-0,1	-0,4	-0,1	-0,4	-0,1	0,6 (**)	-0,1	-0,4
Nanoarchaeaeota	-0,5	0,3	0,5	-0,4	0,4	0,0	0,1	0,0	0,2	0,2	0,4	-0,7 (**)	0,4	-0,2	0,0	0,2	0,1	-0,4
Nitrospinae	-0,3	-0,1	0,1	-0,3	0,0	0,3	0,4	0,3	0,1	0,1	0,3	-0,2	0,1	0,2	0,0	0,1	0,2	-0,1
Nitrospirae	0,3	-0,7	-0,7 (**)	0,4	-0,7 (**)	0,2	0,1	0,2	-0,1	0,0	-0,3	0,4	-0,4	0,4	-0,7 (***)	-0,1	-0,1	0,3
Ochrophyta	-0,2	0,1	0,1	-0,1	0,1	0,3	-0,1	-0,2	0,0	-0,1	-0,2	0,0	0,0	-0,2	-0,2	0,2	-0,2	-0,2
Omnitrophicaeota	-0,5	0,3	0,4	-0,4	0,3	0,0	0,2	0,1	0,2	0,2	0,5 (*)	-0,6 (**)	0,4	-0,1	0,1	0,1	0,3	-0,4
Patescibacteria	0,0	-0,2	-0,1	0,0	-0,2	0,4	0,2	0,2	0,2	-0,1	-0,1	0,1	-0,3	0,2	-0,4	0,2	0,0	0,0
PAUC34f	0,0	-0,1	0,0	0,1	-0,1	0,3	0,4	0,4	0,3	0,1	0,0	-0,1	-0,2	0,3	-0,2	0,2	0,2	0,1
Planctomycetes	0,0	-0,3	-0,3	-0,1	-0,2	0,2	0,4	0,3	0,2	0,3	-0,1	0,2	-0,1	0,2	-0,1	0,2	0,2	0,1
Proteobacteria	0,3	0,2	0,1	0,1	0,1	-0,1	-0,1	-0,1	0,0	-0,1	-0,2	0,3	-0,1	-0,2	0,5	0,0	0,0	0,1
Rokubacteria	0,1	-0,4	-0,5	0,3	-0,4	-0,4	-0,2	0,4	-0,7 (**)	-0,6 (*)	0,1	0,2	0,0	0,7 (*)	-0,3	-0,6 (**)	0,2	0,3
Schekmanbacteria	0,0	-0,3	-0,2	0,1	-0,3	0,3	0,1	0,1	0,2	0,1	-0,1	-0,2	-0,1	0,2	-0,7 (**)	0,2	0,0	0,0
Spirochaetes	-0,4	0,3	0,5	-0,5	0,3	0,5	0,5	-0,2	0,7 (**)	0,6 (*)	-0,1	-0,3	-0,1	-0,6 (*)	0,1	0,8 (***)	-0,2	-0,6
TA06	-0,3	0,0	0,1	-0,3	-0,1	0,3	0,2	-0,1	0,4	0,5	0,0	-0,4	-0,2	-0,1	-0,4	0,4	-0,2	-0,4
Tenericutes	-0,1	0,2	0,1	-0,1	0,1	-0,2	-0,2	-0,2	-0,2	-0,3	0,3	0,0	0,2	0,0	0,1	-0,2	0,0	-0,1
Thaumarchaeota	0,7 (*)	-0,6 (*)	-0,6 (**)	0,6 (*)	-0,6 (**)	0,0	-0,2	0,1	-0,2	-0,3	-0,7 (**)	0,8 (***)	-0,6 (*)	0,3	-0,4	-0,2	-0,3	0,6
Verrucomicrobia	0,5	-0,2	-0,4	0,4	-0,2	-0,4	-0,3	0,3	-0,5 (*)	-0,6 (*)	-0,2	0,4	-0,1	0,4	0,1	-0,6 (*)	0,1	0,5
WS1	-0,3	-0,4	-0,2	-0,2	-0,2	0,3	0,2	0,1	0,3	0,3	-0,1	-0,1	-0,4	0,1	-0,4	0,3	0,1	-0,3
WS2	-0,2	0,0	0,2	-0,1	0,2	0,0	-0,3	-0,1	0,1	0,1	-0,2	-0,1	-0,2	-0,4	0,0	0,1	0,0	-0,2
WS4	-0,2	0,1	0,1	-0,1	0,1	0,3	-0,1	-0,2	0,0	-0,1	-0,2	0,0	0,0	-0,2	-0,2	0,2	-0,2	-0,2
Zixibacteria	-0,3	0,2	0,3	-0,3	0,3	0,1	0,2	0,1	0,1	0,2	0,5	-0,6 (**)	0,4	0,0	0,0	0,2	0,2	-0,2

3
4